USGS
science for a changing world

Characterization and Modes of Occurrence of Elements in Feed Coal and Coal Combustion Products from a Power Plant Utilizing Low-Sulfur Coal from the Powder River Basin, Wyoming

Scientific Investigations Report 2004–5271

U.S. Department of the Interior
U.S. Geological Survey

Characterization and Modes of Occurrence of Elements in Feed Coal and Coal Combustion Products from a Power Plant Utilizing Low-Sulfur Coal from the Powder River Basin, Wyoming

By Michael E. Brownfield, James D. Cathcart, Ronald H. Affolter, Isabelle K. Brownfield, Cynthia A. Rice, Joseph T. O'Connor, Robert A. Zielinski, John H. Bullock, Jr., James C. Hower, and Gregory P. Meeker

Scientific Investigations Report 2004–5271

U.S. Department of the Interior
U.S. Geological Survey

U.S. Department of the Interior
Gale A. Norton, Secretary

U.S. Geological Survey
Charles G. Groat, Director

U.S. Geological Survey, Reston, Virginia: 2005

Posted online July 2005, Version 1.0

This publication is available only online at: http://pubs.usgs.gov/sir/2004/5271/

For more information about the USGS and its products:
Telephone: 1-888-ASK-USGS
World Wide Web: http://www.usgs.gov/

Suggested citation:
Brownfield, M.E., Cathcart, J.D., Affolter, R.H., Brownfield, I.K., Rice, C.A., O'Connor, J.T., Zielinski, R.A., Bullock, J.H., Jr., Hower, J.C., and Meeker, G.P., 2005, Characterization and modes of occurrence of elements in feed coal and coal combustion products from a power plant utilizing low-sulfur coal from the Powder River Basin, Wyoming: U.S. Geological Survey Scientific Investigations Report 2004-5271, 36 p.
Available at URL: http://pubs.usgs.gov/sir/2004/5271/

Contents

Figures

Tables

Characterization and Modes of Occurrence of Elements in Feed Coal and Coal Combustion Products from a Power Plant Utilizing Low-Sulfur Coal from the Powder River Basin, Wyoming

By Michael E. Brownfield, James D. Cathcart, Ronald H. Affolter, Isabelle K. Brownfield, Cynthia A. Rice, Joseph T. O'Connor, Robert A. Zielinski, John H. Bullock, Jr., James C. Hower,[1] and Gregory P. Meeker

Abstract

The U.S. Geological Survey and the University of Kentucky Center for Applied Energy Research are collaborating with an Indiana utility company to determine the physical and chemical properties of feed coal and coal combustion products from a coal-fired power plant. The Indiana power plant utilizes a low-sulfur (0.23 to 0.47 weight percent S) and low-ash (4.9 to 6.3 weight percent ash) subbituminous coal from the Wyodak-Anderson coal zone in the Tongue River Member of the Paleocene Fort Union Formation, Powder River Basin, Wyoming.

Based on scanning electron microscope and X-ray diffraction analyses of feed coal samples, two mineral suites were identified: (1) a primary or detrital suite consisting of quartz (including beta-form grains), biotite, feldspar, and minor zircon; and (2) a secondary authigenic mineral suite containing alumino-phosphates (crandallite and gorceixite), kaolinite, carbonates (calcite and dolomite), quartz, anatase, barite, and pyrite. The primary mineral suite is interpreted, in part, to be of volcanic origin, whereas the authigenic mineral suite is interpreted, in part, to be the result of the alteration of the volcanic minerals. The mineral suites have contributed to the higher amounts of barium, calcium, magnesium, phosphorus, sodium, strontium, and titanium in the Powder River Basin feed coals in comparison to eastern coals.

X-ray diffraction analysis indicates that (1) fly ash is mostly aluminate glass, perovskite, lime, gehlenite, quartz, and phosphates with minor amounts of periclase, anhydrite, hematite, and spinel group minerals; and (2) bottom ash is predominantly quartz, plagioclase (albite and anorthite), pyroxene (augite and fassaite), rhodonite, and akermanite, and spinel group minerals. Microprobe and scanning electron microscope analyses of fly ash samples revealed quartz, zircon, and monazite, euhedral laths of corundum with merrillite, hematite, dendritic spinels/ferrites, wollastonite, and periclase. The abundant calcium and magnesium mineral phases in the fly ash are attributed to the presence of carbonate, clay, and phosphate minerals in the feed coal and their alteration to new phases during combustion.

The amorphous diffraction-scattering maxima or glass "hump" appears to reflect differences in chemical composition of fly ash and bottom ash glasses. In Wyodak-Anderson fly and bottom ashes, the center point of scattering maxima is due to calcium and magnesium content, whereas the glass "hump" of eastern fly ash reflects variation in aluminum content.

The calcium- and magnesium-rich and alumino-phosphate mineral phases in the coal combustion products can be attributed to volcanic minerals deposited in peat-forming mires. Dissolution and alteration of these detrital volcanic minerals occurred either in the peat-forming stage or during coalification and diagenesis, resulting in the authigenic mineral suite.

The presence of free lime (CaO) in fly ash produced from Wyodak-Anderson coal acts as a self-contained "scrubber" for SO_3, where CaO + SO_3 form anhydrite either during combustion or in the upper parts of the boiler. Considering the high lime content in the fly ash and the resulting hydration reactions after its contact with water, there is little evidence that major amounts of leachable metals are mobilized in the disposal or utilization of this fly ash.

Introduction

Coal is likely to remain an important part of the United States energy supply, largely because it is the most abundant, domestically available fossil fuel. One of the major concerns related to the use of coal for electricity production is the release of elements during combustion and the resulting coal combustion products (CCPs)—fly ash and bottom ash—to the environment. This concern and the recent inclusion of

[1]University of Kentucky, Center for Applied Energy Research, Lexington, KY 40511.

coal-fired power plants in the U.S. Environmental Protection Agency (EPA) Toxic Release Inventory (TRI) have prompted the need for accurate, reliable, and quantitative information on the concentration and modes of occurrence of chemical elements in feed coal and CCPs. The TRI is a publicly available EPA database that contains information on toxic chemical releases and other waste management activities reported annually by certain covered industry groups as well as Federal facilities. This inventory was established under the Emergency Planning and Community Right-to-Know Act of 1986 (EPCRA) and expanded by the Pollution Prevention Act of 1990. Many factors contribute to, and control, how coal and coal combustion products will affect the environment and the aqueous solutions that they contact.

The U.S. Geological Survey (USGS), the Kentucky Center for Applied Energy Research, and the Kentucky Geological Survey are collaborating with several electric utilities to determine physical and chemical properties of a variety of feed coals and CCPs from coal-fired electric power plants in Indiana and Kentucky. The long-range goal of the collaborative study is to collect analytical data on the feed coals that will provide a basis for predicting the properties of fly ash produced by the power plants. To accomplish this goal, a team of geologists, geochemists, chemists, coal technologists, and engineers from the USGS, State geological surveys, universities, and electric utility companies was organized to (1) determine the content and modes of occurrence of selected trace elements of the feed coal and the high-volume CCPs; (2) observe variations through time in the properties of CCPs with respect to concurrent variations in the chemical and mineralogical properties of the feed coal; (3) determine the chemistry, mineralogy, magnetic properties, organic properties, and radionuclide content of selected representative samples; and (4) model potential landfill disposal scenarios using batch and flow-through column leaching methods on feed coal and combustion product samples. (See fig. 1.)

In the first phase of the study, the team analyzed coal and CCPs from a Kentucky utility that burns bituminous coal from the Appalachian and Illinois Basins in two power plants. Respective sulfur contents in the coal ranged from 0.6 to 0.9 percent and from 2.5 to 3.5 percent. Much of the data has been released in several reports, including Affolter and others (1997), Breit and others (1996), Brownfield and others (1997), Cathcart and others (1997), Finkelman and others (1996), Finkelman and others (1997), Hower and others (1995), O'Connor (1997a), O'Connor (1997b), Rice and others (1997), Rice and others (1999), and Zielinski and Finkelman (1997). In the second phase of the study, the results of which are the focus of our report, coal and CCPs from an Indiana power plant utilizing low-sulfur (0.23 to 0.47 percent) subbituminous coal from the Wyodak-Anderson zone in the Powder River Basin, Wyo., were similarly analyzed; these analyses provide quantitative data characterizing the physical and chemical properties of the feed coal and combustion products, and give us the means to accurately predict the properties of the fly ash and modes of occurrence of selected trace elements in the fly ash.

Acknowledgments

We are very grateful to Gregory H. Kennan of American Electric Power and Carl Scaggs of the Indiana power plant for providing access to the power plant, providing plant coal and coal combustion product data, and facilitating the sampling at the plant. We have benefited from discussions with American Electric Power and power plant personnel. The authors thank Lorna Carter, Richard Keefer, Richard Pollastro, and Christopher Schenk for their editorial review of the report.

Methodology

Coal is a complex combustible rock made up of organic and inorganic mineral components, each containing many elements. Many factors contribute to, and control, how coal and coal combustion products will affect the environment and the aqueous solutions that they contact. During combustion, elements present in the organic and mineral components of coal are redistributed, as a result of high temperatures, into gaseous and solid-phase reaction products. In the solid-phase reaction products (CCPs), the elements may be uniformly distributed throughout a fly ash grain, enriched in certain grains or areas of grains, or present as coatings, or adsorbed onto fly ash grain surfaces. Particle size, coal rank, amount of ash, coal mineralogy, and trace-element content are important variables controlling the combustion and mobility of elements in coal. For fly ash, the distribution and mobility of elements are influenced by the original composition of the feed coal, the combustion conditions, the size of the fly ash particles, and the fly ash mineralogy. Figure 2 shows various stages in the extraction and utilization of coal that are subject to analytical study.

To characterize the chemistry, mineralogy, and temporal variation of the feed coals and their combustion products, an analytical approach was applied that involved (1) quantitative chemical analysis of feed coal and fly ash; (2) radiographic techniques that quantify the distribution and abundance of radioactive particles; (3) petrographic analysis, X-ray diffraction analysis, and microbeam analysis, including element concentration mapping of small fly ash grains; and (4) analysis of leaching extracts that selectively dissolve certain components of coal or fly ash to simulate environmental conditions (fig. 1).

Sample Collection

The Indiana power plant utilizes a low-sulfur (0.23 to 0.47 weight percent S) and low-ash (5.3 to 6.9 weight percent ash) subbituminous coal from the Wyodak-Anderson coal zone in the Tongue River Member of the Paleocene Fort Union

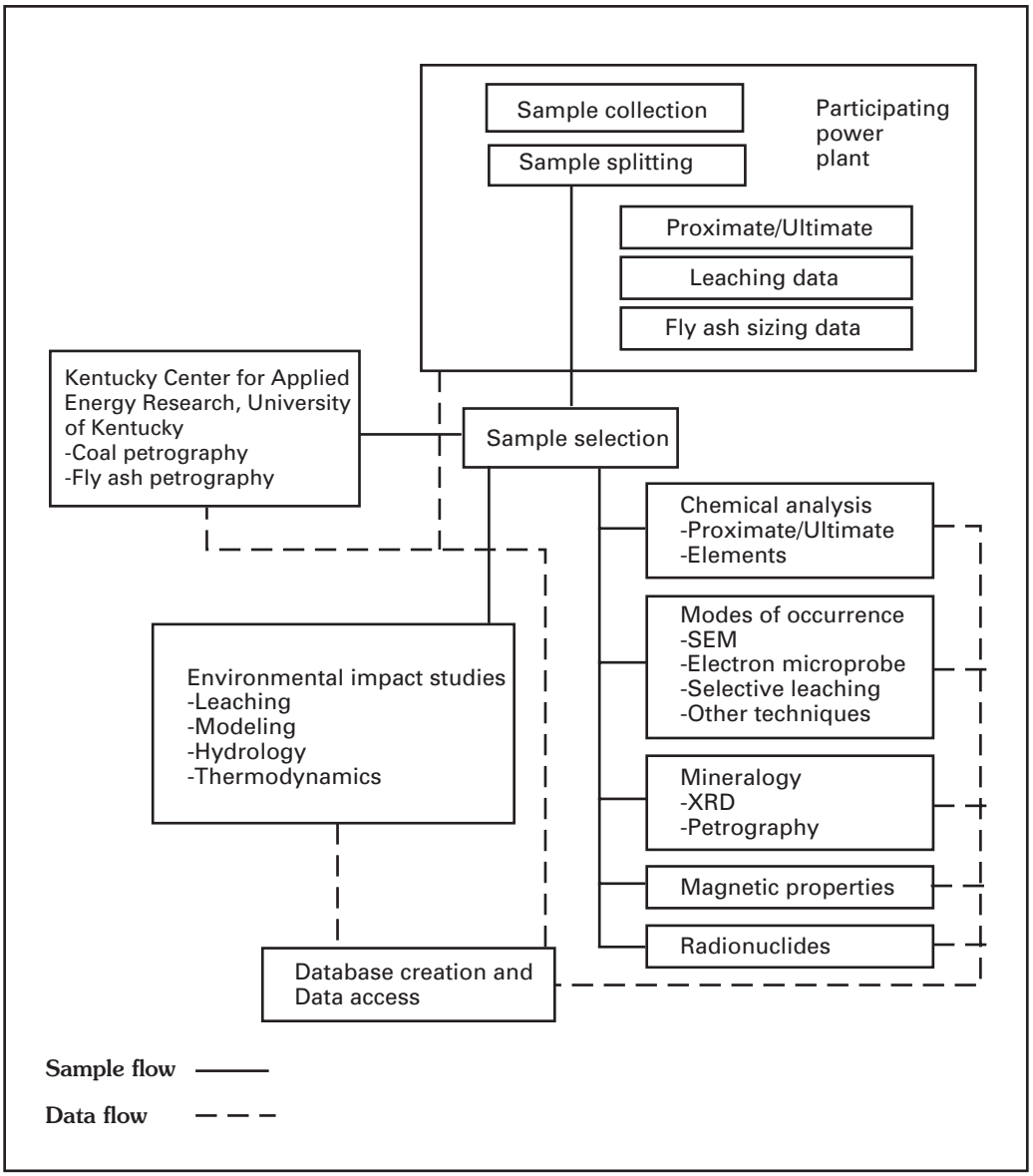

Figure 1. Diagram of sample data flow and sample analysis for the characterization of feed coal, fly ash, economizer ash, and bottom ash.

Formation, Powder River Basin, Wyo. (fig. 3). To determine the temporal variability of feed coal and coal combustion products at this plant, samples were collected daily (15 samples), weekly (14 samples), and monthly (9 samples). Feed coal samples were collected over a 24-hour period from an automated coal collector located before the coal pulverizer after which a representative sample split was prepared at the power plant. Fly ash samples were also collected from automated collectors (old and new samplers) located near the electrostatic fly ash precipitators. The "old sampler" consisted of a 1-in. (inch) pipe, under vacuum, placed in a silo fly ash feed pipe, whereas the "new sampler" consisted of a funnel-shaped pipe, under vacuum, placed in a silo feed pipe. Both devices were designed to collect the fly ash systematically through time. For each sampling, fly ash was collected at four sites in the power plant—one from the economizer (closest to the furnace), two from automated fly ash collectors, and one from a truck storage silo. Power plant personnel collected representative samples of economizer ash, truck fly ash, and bottom ash. Fly-ash sizing data were obtained from the utility operator. During the sampling period, a total of 38 feed coal, 76 fly ash, 38 economizer ash, and 38 bottom ash samples were collected.

Chemical Analysis

Ash yields and major-, minor-, and trace-element contents of feed coal, fly ash, and bottom ash were analyzed in USGS laboratories in Denver, Colo. Coal samples were ashed prior to analysis at 525°C. The presence of most elements was determined by inductively coupled plasma–atomic emission

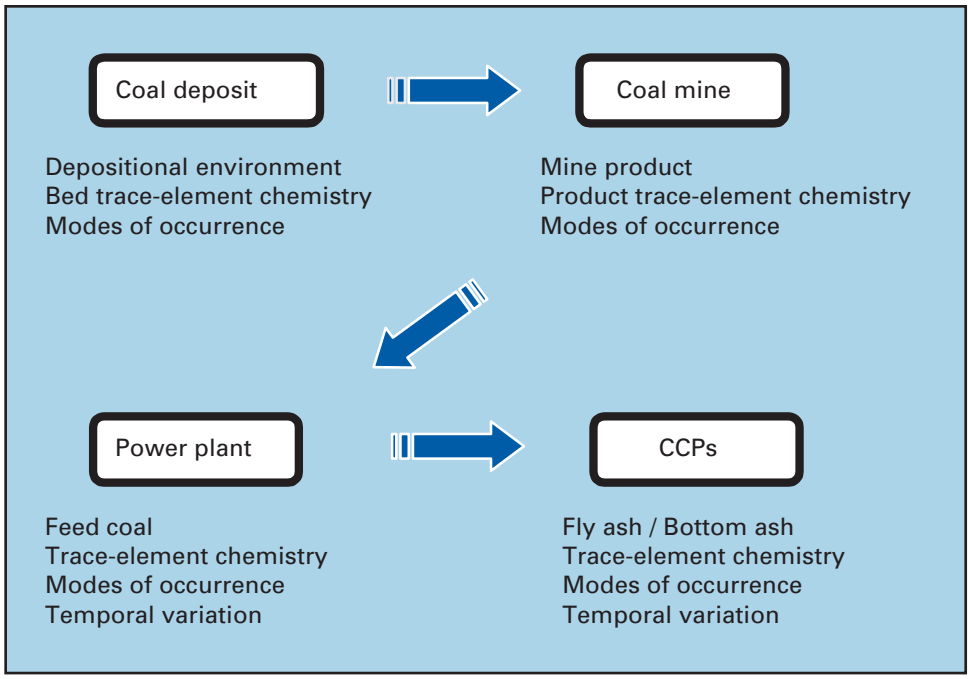

Figure 2. Diagram showing the different data sources with the types of studies and data required to characterize coal and coal combustion products (CCPs).

Figure 3. Upper part of the Wyodak-Anderson coal zone in the Antelope mine, Powder River Basin, Campbell County, Wyo. The Wyodak-Anderson coal zone (as much as 140 ft thick) is the major source of coal in the central Powder River Basin.

spectrometry (ICP-AES) and inductively coupled plasma–mass spectrometry (ICP-MS). Mercury was analyzed by cold vapor atomic absorption spectroscopy (CV-AAS), whereas chlorine content was determined by ion chromatography and selenium was determined by hydride generation atomic absorption. The contents of mercury and selenium in feed coal were determined on sample splits that were not ashed prior to analysis. Proximate, ultimate, and forms-of-sulfur analyses following American Society of Testing and Materials (ASTM) procedures (American Society for Testing and Materials, 1999a) were determined by a commercial laboratory (Geochemical Testing, Inc., Pittsburgh, Pa.).

Radiographic Analysis

The distribution of uranium in individual particles of fly ash and bottom ash was directly observed through use

of fission-track radiography. Polished thin sections of grains of fly ash and bottom ash were prepared and irradiated with neutrons in a research reactor, which induced fission of ^{235}U in the samples. During irradiation, fission fragments recoil from the surface of the thin section and pass into an overlying sheet of muscovite (mica) detector material. The passage of fission fragments causes linear paths of damage or tracks in the mica that are made visible by subsequent etching of the recovered mica in hydrofluoric acid. Areas of high fission-track density in the mica can be related to areas of high uranium concentration in the original sample. Depending upon the angle of incidence, fission-track lengths in the mica are variable, ranging from less than 1 µm (micrometers) to as much as 5 µm. Uraniferous grains or rinds <1 µm thick are magnified by this technique because resulting fission tracks are commonly as much as 5 µm long. Subtler gradients in uranium concentration (less than × 2) can be detected by observing changes in fission-track density across particles greater than 10 µm in diameter.

Petrographic Analysis

Sample splits of feed coal and fly ash were analyzed by the Kentucky Center for Applied Energy Research, which used petrographic microscopy to determine the abundance of major coal macerals in the feed coal and the mineral and amorphous phases in the fly ash. Microscopic analysis of feed coal and fly ash was conducted on ground and polished epoxy-bound pellets (American Society for Testing and Materials, 1999c). The final polishing step used a 0.05-µm alumina slurry. Examination was conducted with reflected-light, oil-immersion optics at a final magnification of × 500–625. Petrographic nomenclature follows the outline of Hower and others (1995) and American Society for Testing and Materials (American Society for Testing and Materials, 1999e).

X-Ray Diffraction Analysis

Coal ash for mineralogical studies was derived by two methods: (1) low-temperature ashing (LTA), and (2) treating the coal with aqueous sodium hypochlorite (NaOCl). Coal samples were ground to –60 mesh and then ashed in a low-temperature plasma asher with radio frequency activated compressed oxygen. During low-temperature ashing, coals were subjected to a maximum ashing temperature of approximately 150°C following procedures of Gluskoter (1965). The NaOCl procedure was modified by Brownfield and others (1995) from Anderson (1963) and Starkey (1984). In this latter procedure, which involved separation of mineral matter from the organic fraction, the coal was first ground to –60 mesh in a ceramic mortar and pestle. The mineral-poor portion of the sample was then separated by flotation methods with carbon tetrachloride (tetrachloromethane, density 1.59 g/cm^3). Approximately 2.5-g units of each mineral-rich sample were placed in 50-mL centrifuge tubes with 5 mL of NaOCl and the pH adjusted to 9.5 by addition of HCl or NaOH. The tubes were heated in a boiling water bath for 10 minutes, then centrifuged at 600 rpm for 8 minutes, and the liquid decanted. Successive treatments were performed (as many as 20) until the supernatant liquid became clear to pale yellow. Distilled water was used to flush the residue into a 500-mL plastic beaker, after which the residue was disaggregated in an ultrasonic generator, and washed and wet-sieved through a 200-mesh screen. Both LTA and NaOCl procedures oxidize and remove organic matter with only minor alteration of the minerals.

Mineralogy of the coal ash, fly ash, and bottom ash samples was determined by X-ray diffraction (XRD) methods. XRD of selected samples was performed on a Phillips XRD 3000 Diffractometer in Bragg-Brentano geometry with Cu Kα radiation (1.5418 Å wave length) scanned at 4°–64° 2θ with a 0.02° stepping increment and a 2-second count scan rate. XRD data were collected digitally and analyzed with Materials Data Inc. (MDI), Livermore, Calif., software and the International Centre for Diffraction Data Power Diffraction File (1999). Magnetic separations (Cathcart and others, 1997) were conducted on some fly and bottom ash samples and the separates were later analyzed by XRD. Relative abundance of minerals was determined using reference intensity methods.

Quantitative mineral data were determined on selected fly ash samples with Rietveld refinement quantitative XRD methods (Larson and Von Dreele, 1994). An internal rutile (TiO_2) standard was added to each sample (0.1 g rutile to 0.9 g of the sample). Rutile was selected because it has a linear absorption coefficient in the mid-range of the phases expected in the sample, therefore minimizing intensity error due to microabsorption (Brindley, 1945). Samples were analyzed on a Phillips Diffractometer using Cu Kα radiation scanned at 20°–80° 2θ with a 0.03° stepping increment and a 2-second count scan rate. XRD data were collected digitally with MDI software, and the publicly available General Structure Analysis System (GSAS) software was used for the Rietveld refinements (Larson and Von Dreele, 1994). Dr. Ryan S. Winburn at Minot State University completed the Rietveld refinements on the fly ash XRD data and reported the quantitative mineral data.

Microbeam Analysis

Samples were prepared and analyzed by microbeam methods using the electron probe microanalyzer (EPMA) and scanning electron microscope (SEM) with energy dispersive X-ray analysis (EDS). Microbeam methods support the mineralogical identifications obtained by X-ray diffraction methods. Feed coal and CCP samples were prepared as polished epoxy-bound sections of the bulk material, whereas low-temperature ash and sodium hypochlorite (NaOCl) treated samples were mounted on conductive carbon tape. Images of the mineral grains were obtained with secondary electron imaging (SEI) and the backscattered electron imaging (BEI) that is responsive to the average atomic number of the imaged object. The SEM analysis was assisted by semiquantitative energy dispersive spectral (EDS) analysis, which allowed the calculation of cation ratios and element contents for many of

the observed phases in the feed coal CCPs. Highly precise chemical compositions (accuracy generally within ±1 percent) were obtained for macrocrystalline phases greater than 5 µm in diameter by means of EPMA wavelength dispersive spectral (WDS) analysis. X-ray intensity mapping was used to collect data on modes of occurrence of selected elements in fly ash and bottom ash grains. Electron microprobe and SEM scans of fly ash grains allowed analysis of samples for relative intensity of individual elements at each counting point. Use of quantitative EPMA with WDS analysis allows as many as five elements per sample to be mapped at one time; SEM element mapping can analyze more elements at one time, but the data are less precise.

Leaching Analysis

Leaching experiments range in duration and severity of chemical treatment. Different types of leaching tests provide different types of information on the leaching behavior of coal and CCPs. Experiments are designed either to simulate a disposal scenario or to selectively dissolve mineral phases. Batch leaching tests combine a solution and a fly ash or coal in a known ratio of solution to material for a selected period of time (seconds to minutes). Solution compositions from the batch tests represent the initial, and commonly highest, concentrations of elements expected to be leached from a material; batch tests are used for regulatory purposes in tests such as the Environmental Protection Agency's Toxicity Characteristic Leaching Protocol (TCLP). Several leaching solution compositions may be used sequentially in these batch tests to dissolve different solid phases. In column leaching experiments, vertical cylinders are filled with fly ash and a solution, such as distilled water, and the solution is allowed to flow through the column. Solutions are collected over the course of the test, which may last several months, and the cumulative amounts of leached elements are determined. Column tests are used to determine long-term (days to months) leaching behaviors of fly ash, simulating the flow of ground or surface water through a material in the natural environment. The material that was leached can also be characterized using XRD or SEM methods to determine any alteration that took place.

Four leaching methods were used in this study for the coal and fly ash samples: 18-hour batch leaches, <1-hour batch leaches, flow-through column leaches, and sequential leaching. A more comprehensive presentation of leaching results from experiments conducted on the Wyodak-Anderson fly ash is underway (C.A. Rice and others, work in progress).

Developing models to predict the behavior of elements during combustion of coal and the potential leaching of CCPs requires quantitative data on the modes of occurrence of those elements in the feed coal. Such data can also be beneficial for evaluation of the environmental impacts, technological impacts, and economic byproduct potential of coal and CCPs. Sequential leaching experiments provide data that determine modes of occurrence of trace elements in feed coal, fly ash, and bottom ash; these data are included herein.

Sequential selective leaching can be used to rapidly determine the modes of occurrence of some inorganic elements in coal (Finkelman and others, 1990) and to support microprobe, SEM, and X-ray diffraction data on these elements. Previous methods to determine the modes of occurrence of elements in coal were labor intensive and provided only limited quantitative data. The most common of these methods included the analysis of density separates of coal (Gluskoter and others, 1977; Querol and others, 1995) and the analysis of size and density separates in low-temperature ash (Palmer and Filby, 1984). Direct methods such as SEM, microprobe, and X-ray diffraction were also used, but were effective only if the element (or mineral) content was above the detection limits.

The sequential leaching procedure used in our study is similar to that described by Finkelman and others (1990) and Palmer and others (2000). For sequential leaching, duplicate 10-g coal samples, ground to –60 mesh, were combined with a solution and agitated for 18 hours, then centrifuged and the leachate separated by filtration. The samples were first leached with 1N ammonium acetate ($NH_4C_2H_3O_2$). This procedure was repeated in subsequent leaching steps using 3N hydrochloric acid (HCl), concentrated (48–51 percent) hydrofluoric acid (HF), and 2N nitric acid (HNO_3). This sequence of solvents was selected so that (1) exchangeable cations, water-soluble compounds, and some carbonates would be removed by $NH_4C_2H_3O_2$; (2) cations associated with carbonates, monosulfides, iron oxides, and chelated organic compounds would be removed by HCl; (3) elements associated with silicates would be removed by HF; and (4) elements associated with disulfides, especially pyrite, would be removed using HNO_3. The sample residue present following the sequential leaching procedure contains the insoluble elements associated with the organic matter and the insoluble or shield minerals.

Trace-element and cation concentrations of the leachates and the final sample residue were determined by inductively coupled atomic emission spectroscopy (ICP-AES) and inductively coupled mass spectroscopy (ICP-MS); anions were determined by ion chromatography (IC). Mercury was analyzed by cold vapor atomic absorption spectroscopy (CV-AAS), whereas selenium was determined by hydride generation atomic absorption.

Results of Analysis

Feed Coal Characterization

Thirty-eight representative feed coal samples were collected at the Indiana power plant. Ten of the feed coal samples collected at the power plant underwent proximate and ultimate analysis, as well as analysis for caloric value, forms of sulfur, and ash-fusion temperatures, following American Society for

Testing and Materials (ASTM) standards methods (American Society for Testing and Materials, 1999a). The feed coal, which was mined from the Wyodak-Anderson coal zone in the Powder River Basin, Campbell County, Wyo., has a mean ash yield of 5.5 percent and a low sulfur (0.3 percent) content (table 1). The apparent rank of the feed coal is within the subbituminous B range (10,395 Btu/lb) using the Parr formula (American Society for Testing and Materials, 1999c), which compares favorably with data reported in the study by Ellis and others (1999) on the Wyodak-Anderson coal.

Coal petrography and vitrinite reflectance data (American Society for Testing and Materials, 1999d) were determined on six sample splits prepared from the feed coal samples collected at the plant by James C. Hower at the Center of Applied Energy Research, University of Kentucky (written commun., 2001) and are shown in table 2. The estimated rank, as determined by the maximum vitrinite reflectance ($R_{o\ max}$; table 2), is not indicative of the calculated subbituminous apparent rank and ranges from lignite to subbituminous (Stach and others, 1982). The feed coal vitrinite reflectance data show a slight distribution of v3 and v4 values (table 2), ranging from 100 percent v3 (0.30–0.39 $R_{o\ max}$) to 65 percent v4 (0.40–0.49 $R_{o\ max}$).

About 40 sample splits from the feed coal samples from the Wyodak-Anderson coal collected from the coal-fired Indiana power plant were prepared by low-temperature ashing (LTA) methods and analyzed by XRD. X-ray diffraction analyses of the coal LTA ash (fig. 4) reveal a predominance of well-crystallized kaolinite ($Al_2Si_2O_5(OH)_4$) and quartz (SiO_2). Scanning electron microscope and XRD analysis of the feed coal, coal ash (table 3), and NaOCl-treated coal revealed minor amounts of hydrated alumino-phosphate minerals (figs. 5 and 6) containing Ba, Ca, and Sr, and trace amounts of beta-form quartz (fig. 7), apatite ($Ca_5(PO_4)_3F$), zircon ($ZrSiO_4$; fig. 8), plagioclase (albite, $NaAlSi_3O_8$), and potassium feldspar (sanidine, $(K,Na)AlSi_3O_8$). The hydrated aluminum-phosphates were grouped by Palache and others (1951) as the plumbogummite group and later regrouped by Fleischer (1987) as the crandallite group. Fleischer's classification is used in this report; the general formula for the crandallite group is $XAl_3(PO_4)_2(OH)_5{\cdot}H_2O$. The minerals identified include crandallite (X=calcium) and gorceixite (X=barium), which are commonly in a solid solution state rather than representing pure end members, and they may contain trace amounts of Sr, Ce, and Pb. Other minerals identified in the NaOCl-treated feed coal include rounded grains of detrital quartz, calcite ($CaCO_3$), dolomite ($CaMg(CO_3)_2$), siderite ($FeCO_3$), ankerite ($Ca(Fe,Mg,Mn)(CO_3)$), iron oxide (hematite, α-Fe_2O_3), biotite ($KX_3AlSi_3O_{10}(OH)_2$, where X=Fe and (or) Mg), muscovite ($KAl_2(Si_3Al)O_{10}(OH,F)_2$), anatase ($TiO_2$), barite ($BaSO_4$), pyrite ($FeS_2$), rutile ($TiO_2$), chromite ($FeCr_2O_4$), monazite ($(RE,Th)PO_4$, where RE=rare earth elements Ce, La, Nd), ilmenite ($FeTiO_3$), and cerussite ($PbCO_3$).

Two mineral suites were identified in the feed coal from the Wyodak-Anderson coal: a primary detrital suite and an authigenic suite. The primary detrital suite consisted of quartz (detrital and volcanic beta-form grains), biotite, apatite, potassium feldspar (sanidine?), plagioclase (albite?), zircon, rutile, ilmenite, chromite, and monazite. Quartz grains in this suite are primarily clear, colorless, and angular; flake and blade shapes are common with minor frosted and rounded grains, which may be of windblown origin. Sharp euhedral (fig. 7) to rounded beta-form quartz bipyramids are also present, a few of which display pitting along the hexagonal bipyramids and authigenic quartz overgrowth on the prism faces (fig. 9). Biotite and muscovite are generally in the form of irregular flakes some of which display dissolution along their edges. Pseudo-hexagonal biotite crystals were also observed. Zircon is represented by euhedral prismatic crystals terminated by pyramids in NaOCl-treated coal samples; both doubly terminated and broken crystals with only one or no terminations were observed. Potassium feldspar (fig. 10) and plagioclase (fig. 11) are mostly angular cleavage fragments in the NaOCl-digested coal samples.

An authigenic mineral suite consisted of kaolinite, alumino-phosphates (crandallite, fig. 5; gorceixite, fig. 6), calcite (fig. 12), dolomite (fig. 13), siderite, ankerite, anatase (fig. 14), quartz (fig. 15), barite, iron oxide (hematite, fig. 16), and pyrite. In polished coal mounts, kaolinite occurs in plant-cell fillings and irregular masses within thin zones of mineral matter. Crystallized kaolinite was observed in the low-temperature ash samples. The alumino-phosphate minerals were also observed, filling plant cells (fig. 5) and as subhedral crystals (fig. 6) in the NaOCl-digested coal samples. Authigenic quartz was observed as quartz overgrowths on the beta-form quartz grains (fig. 9) and as quartz casts replacing plant material (fig. 15) in the digested coal samples. Carbonate minerals (calcite, dolomite, siderite, ankerite) are mostly subhedral grains and rhombohedral cleavage fragments (figs. 12 and 13). Barite was noted in polished mounts as cell fillings and as subhedral cleavage fragments in the digested coal samples. Iron oxide, possibly hematite, was abundant in the NaOCl-treated samples, forming irregular masses and spheres (fig. 16) that most likely represent fecal pellets. Pyrite was observed as irregular flat grains, probably representing cleat fillings, and as small framboids.

Major and minor oxide contents for the feed coal from the Wyodak-Anderson coal are shown in table 4. Trace elements of environmental interest as defined by the 1990 Clean Air Act Amendments (U.S. Statutes at Large, 1990) for the Wyodak-Anderson feed coal are shown in table 5. Results of chemical analyses show minor differences in the compositions of the feed-coal stocks. A more complete report of temporal variation of the Wyodak-Anderson feed coal is underway (R.H. Affolter and others, work in progress).

Leaching and Modes of Occurrence of Selected Elements in Feed Coal

Three feed-coal samples were sequentially leached with 1N ammonium acetate ($NH_4C_2H_3O_2$), 3N hydrochloric acid

Table 1. Mean values for proximate and ultimate analysis, caloric value, forms of sulfur, and ash-fusion temperatures of 10 samples of Indiana power plant feed coal mined from the Wyodak-Anderson coal zone, Powder River Basin, Wyo.

[All samples on an as-received basis]

	Mean	Median	Range		Standard deviation
			Minimum	Maximum	
Proximate and ultimate analysis (percent)					
Moisture	17.1	17.4	8.3	23.3	5.4
Volatile matter	36.7	36.5	34.2	39.1	1.6
Fixed carbon	40.6	40.8	36.3	46.7	3.4
Ash	5.5	5.4	4.9	6.3	0.4
Hydrogen	6.0	5.9	5.4	6.5	0.4
Carbon	57.4	57.0	52.8	64.0	3.7
Nitrogen	0.7	0.7	0.6	0.9	0.1
Oxygen	30.1	30.7	23.0	35.0	3.9
Sulfur	0.34	0.33	0.23	0.47	0.1
Caloric value					
Btu/lb	9,790	9,700	9,060	10,780	600
Forms of sulfur (percent)					
Sulfate	0.02	0.02	0.01	0.03	0.01
Pyritic	0.04	0.04	0.04	0.05	0.0
Organic	0.28	0.26	0.17	0.39	0.09
Ash-fusion temperatures (°F)					
Initial deformation	2,060	2,065	2,020	2,080	19
Softening temperature	2,090	2,090	2,060	2,150	26
Hemispherical temperature	2,110	2,105	2,090	2,160	21
Fluid temperature	2,130	2,125	2,100	2,170	23

(HCl), concentrated hydrofluoric acid (HF), and 2N nitric acid (HNO_3). The leachates were analyzed and the chemical data were processed to obtain the percentages for each element leached by the four solvents. The calculated percentages were used as a semiquantitative measure of the modes of occurrence of the elements. A comparison of quality control data from standards with data from the leachates indicated an estimated error of plus or minus 20 percent for this study. Table 6 shows concentrations of selected elements resulting from the sequential leaching experiments on Wyodak-Anderson coal samples. (See table 9 for modes of occurrence for selected elements.)

The selective leaching results indicate that 40 percent or more of the elements Ba, Co, Fe, Mn, P, Pb, Sr, Th, and U are associated with HCl-soluble compounds (table 6) such as carbonates, monosulfides, and oxides, whereas 40 percent or more of the elements As, Co, Cr, Ni, Se, and Zn are associated with insoluble phases or with organic matter. All of the mercury in the Wyodak-Anderson coal samples appears to be organically associated. Portions of the elements Be, Cr, Se, Th, and U are associated with HF and HNO_3 soluble compounds, including clays and other silicates and pyrite and other disulfides.

Coal Combustion Products

More than 150 fly ash samples, produced from combustion of feed coal from the Wyodak-Anderson coal zone, Powder River Basin, Wyo., were collected and analyzed by X-ray diffraction (fig. 17; table 3). X-ray diffraction data revealed a predominance of aluminate glass, merwinite ($Ca_3Mg(SiO_4)_2$), lime (CaO), and gehlenite ($Ca_2Al(Al,Si)O_7$) with minor and trace amounts of quartz, apatite, anhydrite ($CaSO_4$), hematite (α-Fe_2O_3), periclase (MgO), perovskite ($CaTiO_3$), magnesioferrite ($MgFe_2^{3+}O_4$), and magnetite ($Fe^{2+}Fe_2^{3+}O_4$). Periclase and lime were detected in all samples except the economizer fly ash (fig. 18). Gehlenite forms a solid solution series with akermanite ($Ca_2MgSi_2O_7$) and melilite ($(Ca,Na)_2(Al,Mg)(Si,Al)_2O_7$), which were found in trace amounts. A comparison among the fly ash samples showed gehlenite to be more abundant in the economizer ash, whereas perovskite was more abundant in the fly ash samples collected from the precipitators. Anhydrite forms thin coatings on many of the fly ash grains. Rietveld X-ray diffraction analysis conducted on three samples (table 7) confirmed that glass, merwinite, gehlenite, and quartz were the predominant phases with minor and trace amounts of C3A (a concrete industry abbreviation for a calcium aluminate, $Ca_3Al_2O_6$), anhydrite, periclase, hematite, lime, and magnetite. Petrographic analysis confirmed the presence of minor amounts of mullite, quartz, and spinel/ferrite (table 8) with traces of coke and inertinite (James C. Hower, written commun., 2001).

Microprobe and SEM analysis of fly ash samples detected mineral grains that were consistent with quartz, zircon, monazite, euhedral laths of corundum, merwinite, hematite, dendritic spinels and ferrites, and rounded grains of

Table 2. Petrology and vitrinite reflectance of an Indiana power plant feed coal from the Wyodak-Anderson coal zone, Powder River Basin, Campbell County, Wyo.

[Data from James C. Hower, Center for Applied Energy Research, University of Kentucky, Lexington, Ky., written commun., 2001. t, trace amount; R_{max}, mean maximum reflectance measured in oil; s.d., standard deviation; v3, percent of values from 0.30-0.39; v4, percent of values from 0.40-0.49; n.d., not determined, humic macerals not suitable for reflectance measurements]

Sample	Macerals and petroleum coke (Pet coke), in percent										
	Vitrinite				Liptinite		Inertinite				Pet coke
	Ulminite	Textinite	Humodetrinite	Corpocollinite	Exinite	Resinite	Fusinite	Semifusinite	Micrinite	Macrinite	
RP1	26.0	26.0	22.4	4.0	4.2	0.8	11.8	4.8	0.0	0.0	0.0
RP4	30.2	20.8	27.2	5.6	5.6	2.4	5.2	3.0	t	t	0.0
RP14	23.4	23.6	29.4	7.2	2.2	0.6	9.8	3.6	0.2	0.0	0.0
RP17	33.0	18.4	25.4	6.2	4.6	0.6	8.0	3.8	0.0	t	0.0
RP20	30.8	16.8	29.4	2.8	2.6	1.4	11.2	4.4	0.0	0.6	0.0
RP29	25.8	24.3	30.6	6.9	0.6	0.2	8.5	2.7	0.2	0.0	0.2

Sample	Vitrinite reflectance (oil-immersion, 500X)			
	R_{max}	s.d.	v3	v4
RP1	0.39	0.03	57	43
RP4	0.38	0.03	76	24
RP14	n.d.	n.d.	n.d.	n.d.
RP17	0.40	0.03	35	65
RP20	0.40	0.02	36	64
RP29	0.35	0.02	100	0.0

wollastonite ($CaSiO_3$) with periclase. The composition of the associated glass was somewhat variable but generally consisted of calcium and aluminum with minor and trace amounts of Si, Fe, Mg, Ti, Na, K, P, and As (O'Connor and Meeker, 1999).

A small percentage of fly ash grains (<5 percent) are composed of cryptocrystalline phosphorus phases with whitlockite ($Ca_9(Mg, Fe^{+2})(PO_4)_6(PO_3(OH))$ and its anhydrous analog merrillite, or α-$Ca_3(PO_4)_2$, as the most likely mineral phases (O'Connor and Meeker, 1999).

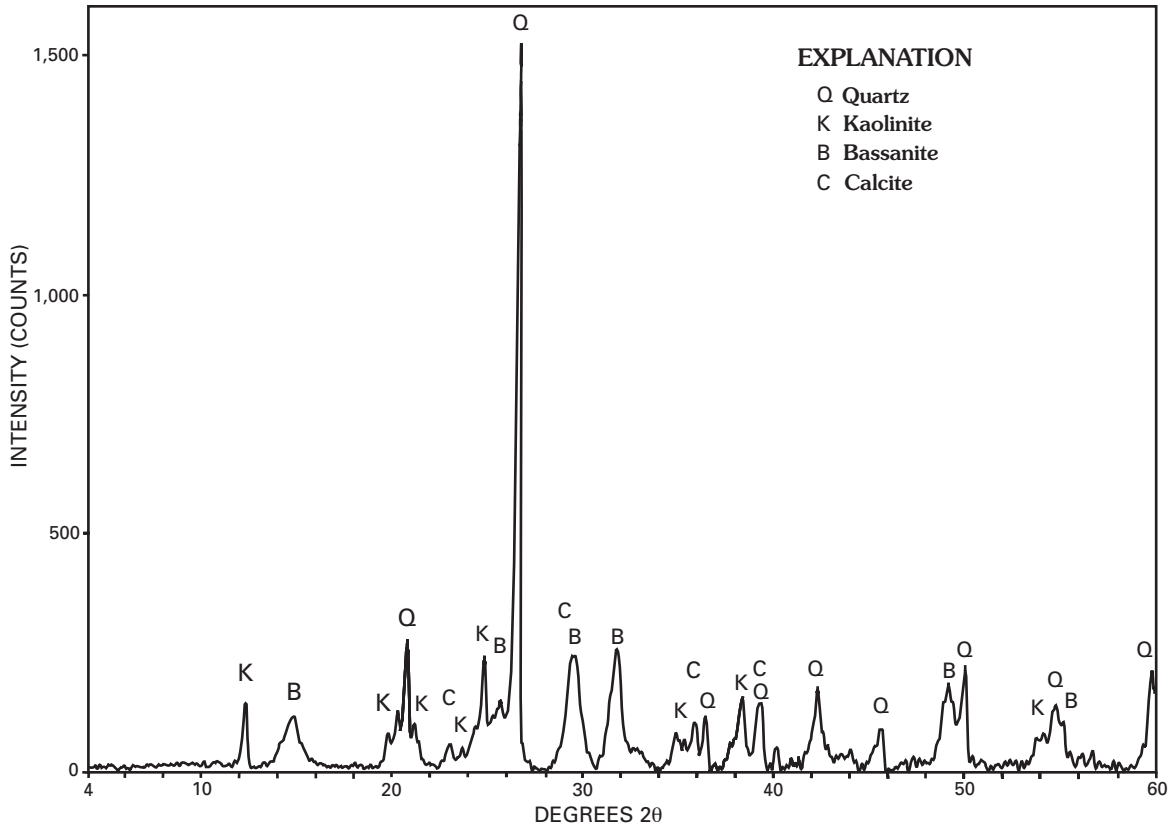

Figure 4. X-ray diffractogram of low-temperature ash (LTA) from a power plant feed coal mined from the Wyodak-Anderson coal zone, Powder River Basin, Wyo.

Table 3. Results of X-ray diffraction, SEM, and microprobe analysis of feed coal, fly ash, and bottom ash from an Indiana power plant utilizing coal from the Wyodak-Anderson coal zone, Powder River Basin, Wyo.

[Feed coal mineralogy determined from low-temperature ash, NaOCl-treated samples, and polished pellets. Mineral formulas from Fleischer (1999). Minerals are listed in order of relative abundance. Ma, major (> 10 percent); Mi, minor (5-10 percent); T, trace (< 5 percent)]

Feed coal	Fly ash	Bottom ash
Quartz SiO_2 alpha form – Ma	Glass – Ma	Glass – Ma
Kaolinite $Al_2Si_2O_5(OH)_4$ – Ma	Merwinite $Ca_3Mg(SiO_4)_2$ – Ma	Quartz – Mi
Calcite $CaCO_3$ – T	Gehlenite $Ca_2Al(Al,Si)O_7$ – Mi	Anorthite $CaAl_2Si_2O_8$ – Mi
Biotite and muscovite(?) – T	Quartz – Mi	Augite $(Ca,Na)(Mg,Fe,Al,Ti)(Si,Al)_2O_6$ – Mi
Crandallite group – T	Anhydrite $CaSO_4$ – T	Fassaite Fe-Al diopside or augite – Mi
Plagioclase albite – T	[1]C3A $Ca_3Al_2O_6$ – T	Rhodonite $(Mn^{2+},Fe^{2+},Mg,Ca)SiO_3$ – Mi
Potassium feldspar – T	Apatite $Ca_5(PO_4)_3F$ – T	Akermanite $Ca_2MgSi_2O_7$ – T
Hematite α-Fe_2O_3 – T	Periclase MgO – T	Melilite $(Ca,Na)_2(Al,Mg)(Si,Al)_2O_7$ – T
Quartz SiO_2 beta-form – T	Mullite $Al_6Si_2O_{13}$ – T	Albite $(NaAlSi_3O_8)$ – T
Dolomite $CaMg(CO_3)_2$ – T	Lime CaO – T	Magnetite $Fe^{2+}Fe_2^{3+}O_4$ – T
Anatase TiO_2 – T	Magnesioferrite $MgFe_2^{3+}O_4$ – T	Magnesioferrite $MgFe_2^{3+}O_4$ – T
Barite $BaSO_4$ – T	Hematite α-Fe_2O_3 – T	Pyrite – T
Pyrite FeS_2 – T	Perovskite $CaTiO_3$ – T	Anhydrite – T
Zircon $ZrSiO_4$ – T	Akermanite $Ca_2MgSi_2O_7$ – T	Zircon – T
Apatite $Ca_5(PO_4)_3F$ – T	Melilite $(Ca,Na)_2(Al,Mg)(Si,Al)_2O_7$ – T	
Siderite $FeCO_3$ – T	Whitlockite $Ca_9(Mg, Fe^{+2})(PO_4)_6(PO_3,OH)$ – T	
Ankerite $(Ca(Fe,Mg,Mn)(CO_3)_2)$–T	Merrillite α-$Ca_3(PO_4)_2$ – T	
Cerussite $(PbCO_3)$	Magnetite $Fe^{2+}Fe_2^{3+}O_4$ – T	
Monazite $(RE,Th)PO_4$ – T		
Ilmenite $FeTiO_3$ – T		

[1]C3A is a concrete industry abbreviation for a calcium aluminate, $Ca_3Al_2O_6$.

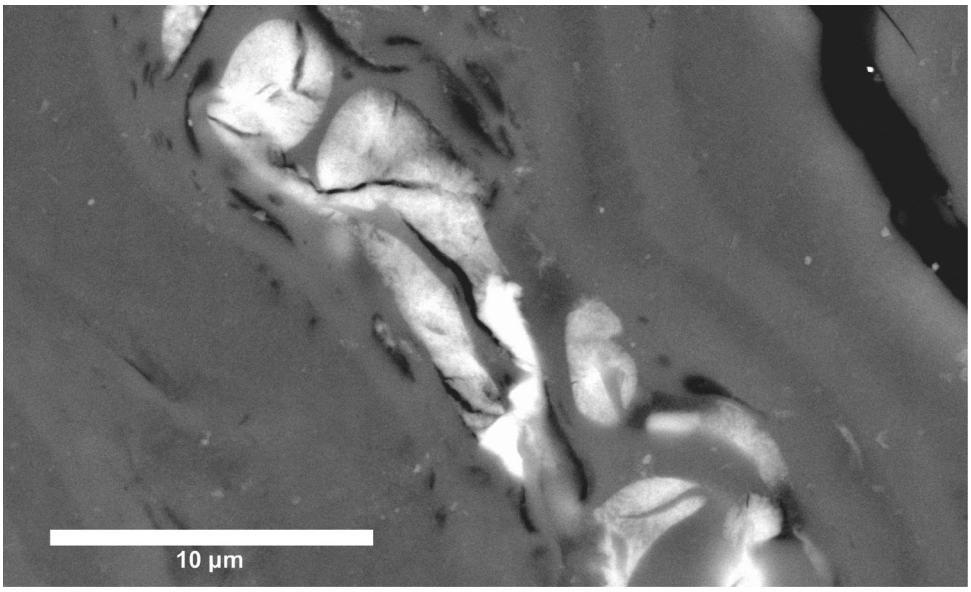

Figure 5. Scanning electron microscope (SEM) secondary electron image of hydrated alumino-phosphate (crandallite) filling plant cells, from an Indiana power plant feed coal from the Wyodak-Anderson coal zone, Powder River Basin, Wyo.

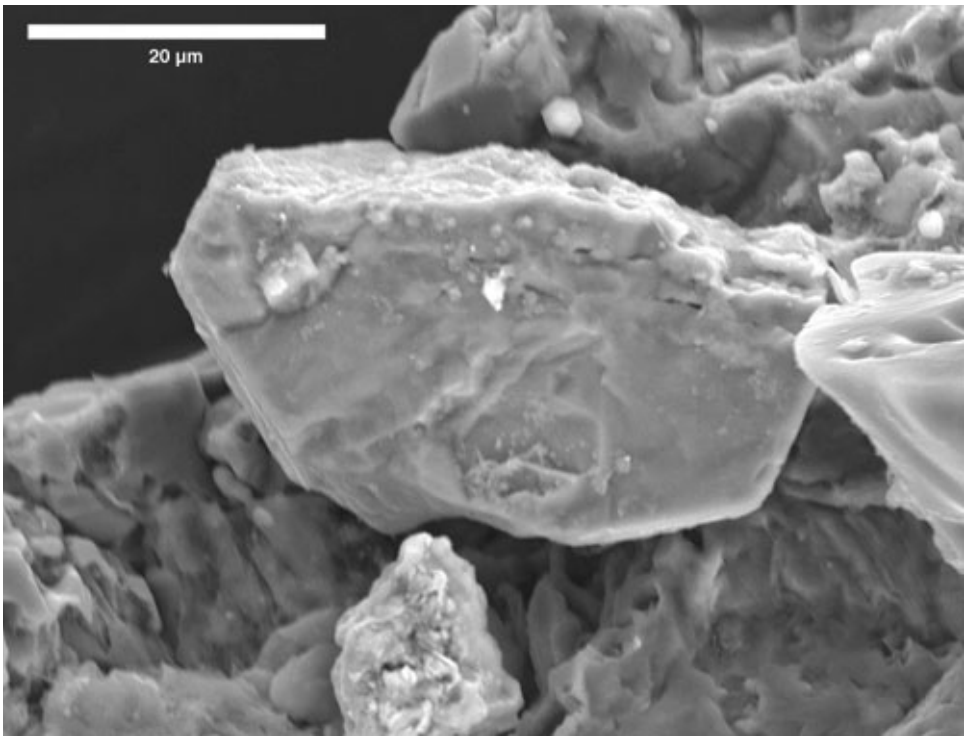

Figure 6. Scanning electron microscope (SEM) secondary electron image of a subhedral crystal of gorceixite ($BaAl_3(PO_4)_2(OH)_5 \cdot H_2O$), from an Indiana power plant feed coal from the Wyodak-Anderson coal zone, Powder River Basin, Wyo.

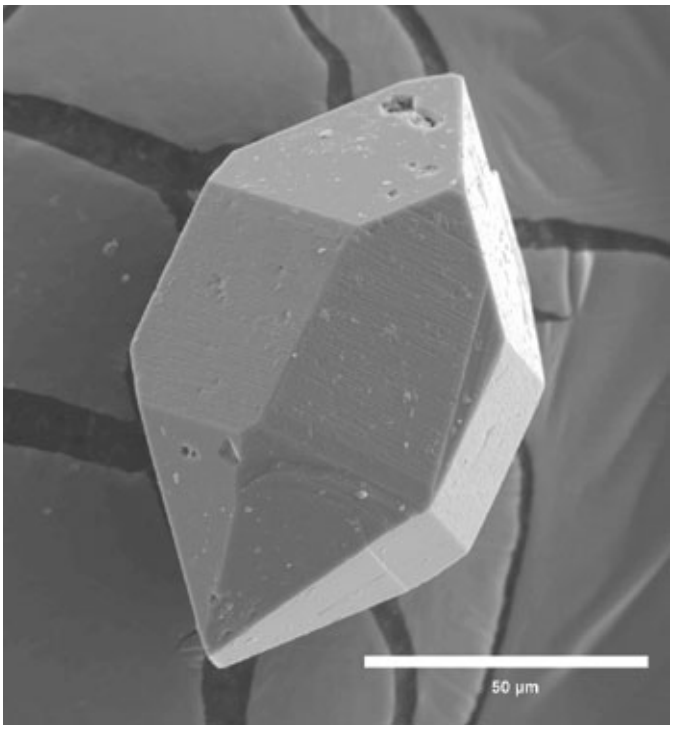

Figure 7. Scanning electron microscope (SEM) secondary electron image of a euhedral crystal of beta-form quartz, from an Indiana power plant feed coal from the Wyodak-Anderson coal zone, Powder River Basin, Wyo.

Fly ash samples were also collected and analyzed from an abandoned surface disposal site from which the ash was being processed as soil amendment. The material had been subjected to natural precipitation as well as water used for dust suppression. X-ray diffraction analysis revealed major amounts (> 10 percent) of chabazite $(Ca,K,Na)_4Al_4Si_8O_{24}\cdot 12H_2O$), ettringite $(Ca_6Al_2(SO_4)_3(OH)_{12}\cdot 26H_2O)$, and strätlingite $(Ca_8Al_4(Al_4Si_4)O_8(OH)_{40}\cdot 10H_2O)$ and lesser amounts (<10 percent) of calcite, C3A, gehlenite, merwinite, mullite, quartz, thaumasite $(Ca_6Si_2(CO_3)(SO_4)_2(OH)_{12}\cdot 24H_2O)$, and hematite. Chabazite, ettringite, strätlingite, thaumasite, and calcite are authigenic mineral phases resulting from alteration of the original fly ash.

The magnetic fraction recovered from fly ash samples from combusted Wyodak-Anderson coal in our study ranges from 1.0 to 2.0 percent; it consists of dendritic magnetite and magnesioferrite and subhedral to euhedral hematite (table 3). The small percentage of magnetic minerals is the result of the low pyrite content of the feed coal when compared to Appalachian Basin and Illinois Basin feed coals (Brownfield and others, 1997; Brownfield, Affolter, Cathcart, O'Connor, and Brownfield, 1999). Magnetic minerals in fly ash have been described as magnetite, ferrites, and hematite (Lauf and others, 1982; Brownfield and others, 1997; Cathcart and others, 1997).

X-ray diffraction analysis of 38 samples of the Wyodak-Anderson bottom ash (fig. 19) revealed quartz, plagioclase (anorthite), and pyroxene (augite and fassaite) with minor and trace amounts of rhodonite, akermanite, melilite, pyrite, and anhydrite (table 3). All samples contained some amorphous aluminum silicate glasses, char (unburned coal), sulfate minerals, and illite and (or) muscovite. Analysis of samples by SEM detected detrital grains of quartz and zircon and high-aluminum pyroxene (fassaite) laths with anorthite (fig. 20). The composition of the associated bottom ash glass was variable in composition but generally consisted of Ca and Al with minor and trace amounts of Si, Fe, Mg, Ti, and Na. The bottom ash contains less Ca and Mg when compared to the fly ash (table 4).

X-Ray Element Mapping

Quantitative, element intensity mapping via the electron microprobe provides relative intensities of individual elements at each counting point and helps to develop a better understanding of modes of occurrence and potential release of selected elements to the environment. For example, figure 21 shows a backscattered electron image and three element maps (Cr, Ni, and Si) of a fly ash grain from a Kentucky power plant. The images reveal a distinct enrichment of nickel but a lesser amount of chromium in both the glassy and ferrite portions of the grain (Robert B. Finkelman, written commun., 2002). Figure 22 shows a second example of a backscattered electron image and three elements maps (Ca, Mg, and S) of a fly ash grain with a distinct rim of calcium and sulfur resulting from a thin anhydrite ($CaSO_4$) coating on a power plant fly ash grain (Brownfield, Affolter, Cathcart, O'Connor, and Brownfield, 1999). The bright areas in the center of the Mg element map are small periclase crystals (MgO) in a Ca-aluminate. Electron microprobe element intensity mapping is limited to elements that are present at or above the detection limits of the microprobe (approximately 0.1 weight percent). Attempts to map elements of environmental interest (U.S. Statutes at Large, 1990) in Wyodak-Anderson fly ash grains (table 5) were not successful because the elements were all near or below detection limits of the microbeam instruments. Element intensity mapping is still a valuable tool in determining modes of occurrence of other elements in coal combustion products.

Discussion and Interpretation

Determination of elements in feed coal is important because the content, distribution, and behavior of elements during and after combustion largely reflect the content and distribution of trace elements in the feed coal. Elements of environmental interest as defined by the 1990 Clean Air Act Amendments (U.S. Statutes at Large, 1990) are doubly important because they can be potentially released into the environment during coal utilization.

In our study, samples of the Wyodak-Anderson coal used as feed coal contained higher Ba, Ca, Mg, Na, P, Sr, and Ti contents than the eastern feed coals that were studied by

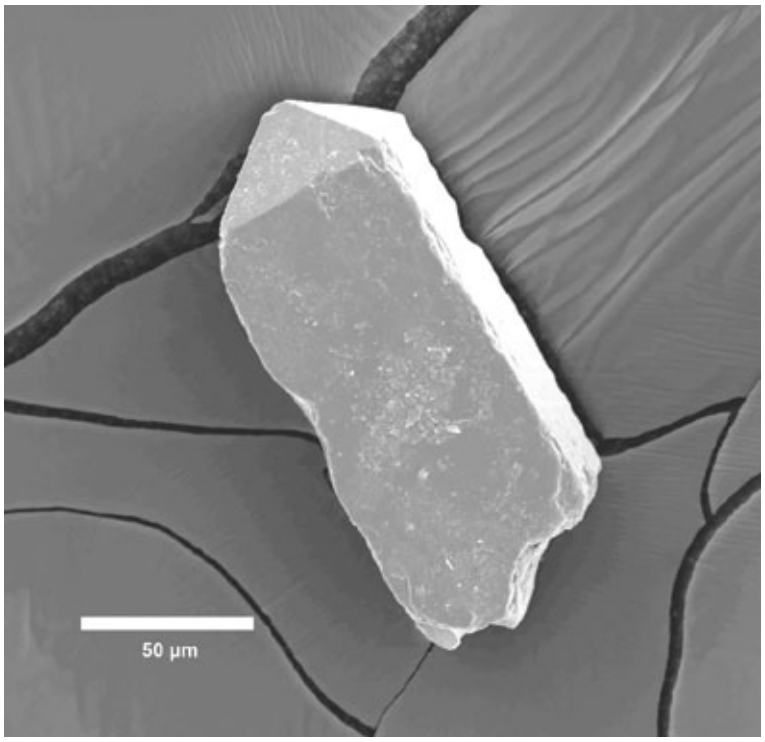

Figure 8. Scanning electron microscope (SEM) secondary electron image of a euhedral crystal of zircon, from an Indiana power plant feed coal from the Wyodak-Anderson coal zone, Powder River Basin, Wyo.

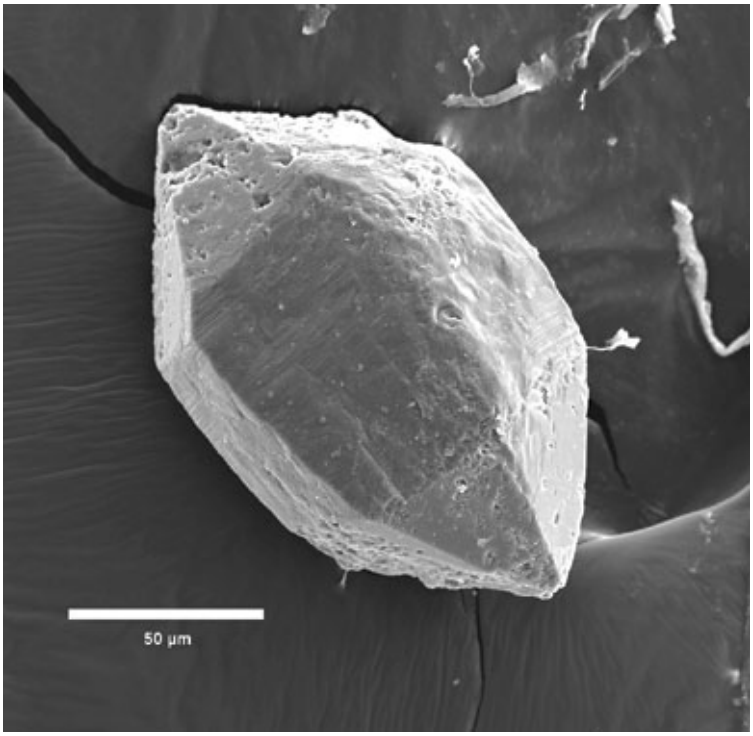

Figure 9. Scanning electron microscope (SEM) secondary electron image of a euhedral crystal of beta-form quartz, from an Indiana power plant feed coal from the Wyodak-Anderson coal zone, Powder River Basin, Wyo. The crystal has been partially etched on its hexagonal pyramids and shows authigenic quartz overgrowth on its prism faces.

Brownfield, Affolter, Cathcart, O'Connor, and Brownfield (1999). These elements are associated with the minerals crandallite (Ba, Ca, P, and Sr), gorceixite (Ba, Ca, P, and Sr), biotite (Ba and Ca), calcite (Ba, Ca, and Sr), and clay minerals (Ca and Mg). They are indicative of coals containing altered airfall volcanic ash (Affolter and Brownfield, 1987; Brownfield and Affolter, 1988; Affolter and others, 1997). In low-rank Powder River Basin coals, major portions of the total Ca and Mg contents are associated with the organic matter as a result of cation exchange. Additionally, detrital mineral input and mineral enrichment as a result of epigenetic ground-water flow have contributed to the geochemical makeup of the feed coal.

The Wyodak-Anderson coal, although mined in several mines in the eastern Powder River Basin, displayed little variation in element content during its first 15-day sampling

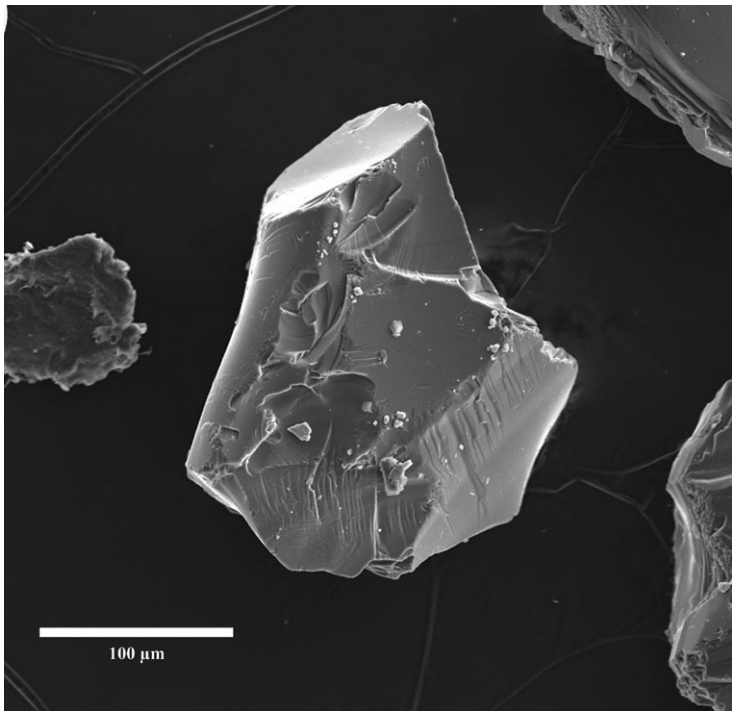

Figure 10. Scanning electron microscope (SEM) secondary electron image of an irregular cleavage fragment of potassium feldspar (sanidine?), from an Indiana power plant feed coal from the Wyodak-Anderson coal zone, Powder River Basin, Wyo.

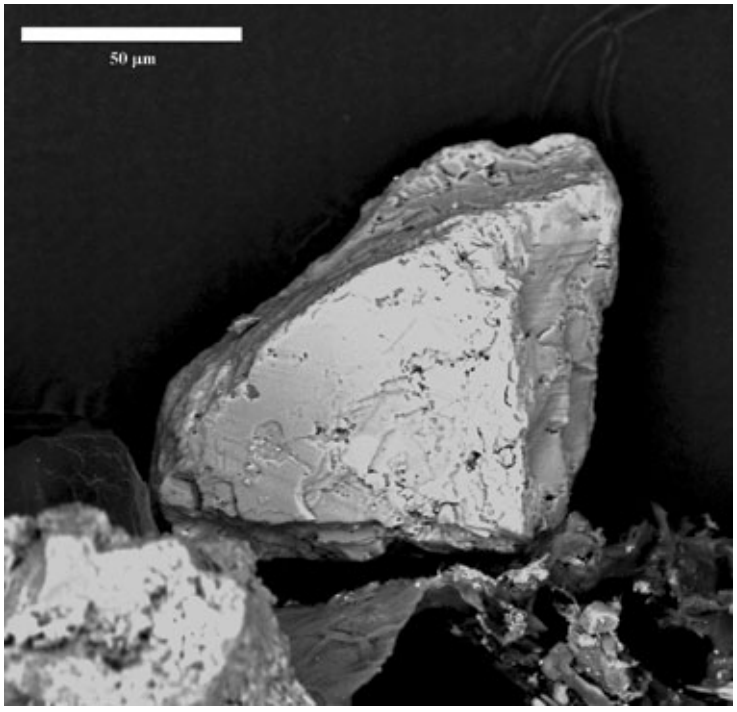

Figure 11. Scanning electron microscope (SEM) secondary electron image of an irregular cleavage fragment of plagioclase feldspar (albite?), from an Indiana power plant feed coal from the Wyodak-Anderson coal zone, Powder River Basin, Wyo.

period as feed coal at the Indiana power plant (Affolter and others, 1999). In general, the Wyodak-Anderson coal displays little variation in the standard deviation with respect to the proximate and ultimate analysis (table 1) of ash and sulfur during the sample period. However, minor trace-element variation can occur within the Wyodak-Anderson coal zone, which is as much as 140 ft thick, as the result of both vertical and lateral changes in mineral content and the amount of individual mineral phases within the coal bed at the different mines. Examples of minor variations in trace-element content are shown in figures 23 and 24, which display the maximum, minimum, and mean contents of Ba and P as determined for

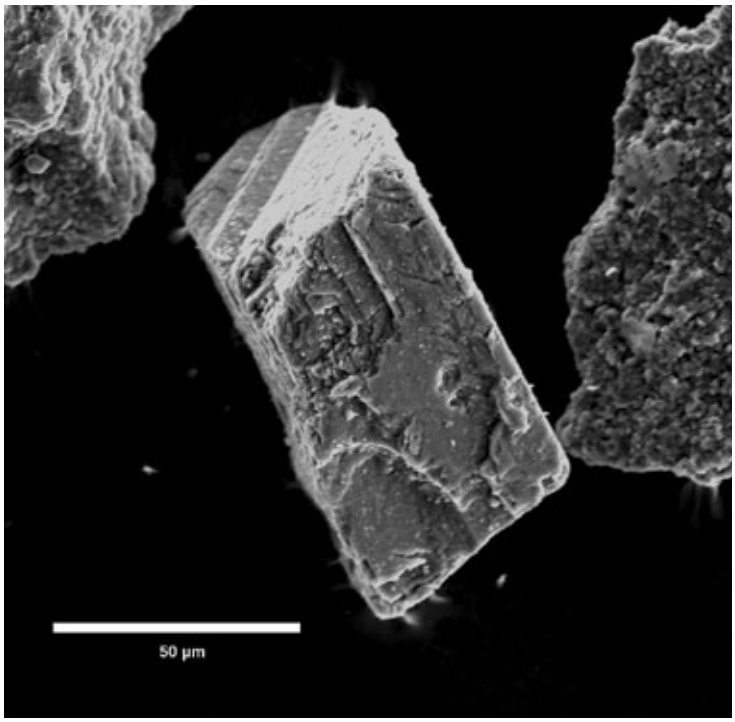

Figure 12. Scanning electron microscope (SEM) secondary electron image of a subhedral crystal of calcite ($CaCO_3$), from an Indiana power plant feed coal from the Wyodak-Anderson coal zone, Powder River Basin, Wyo.

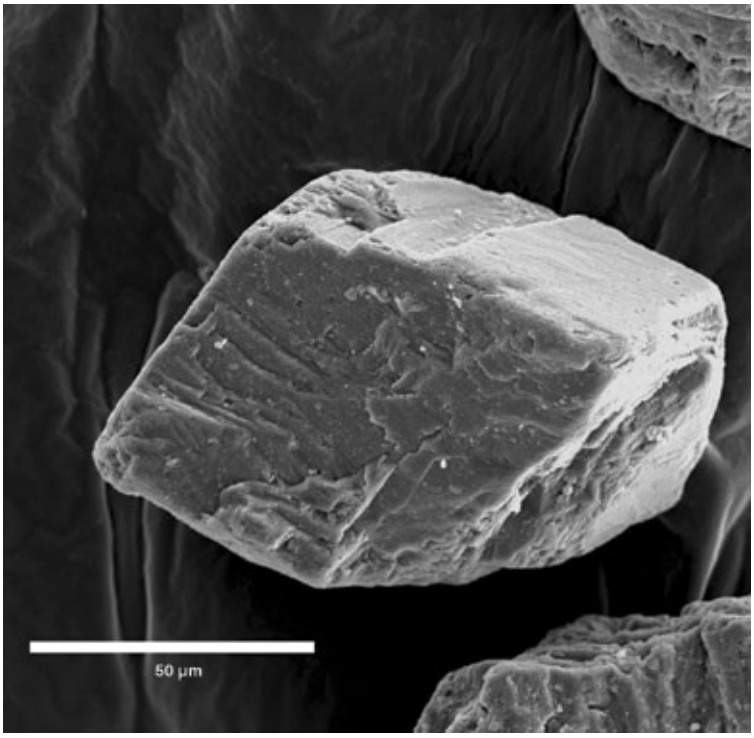

Figure 13. Scanning electron microscope (SEM) secondary electron image of a subhedral crystal of dolomite ($CaMg(CO_3)_2$), from an Indiana power plant feed coal from the Wyodak-Anderson coal zone, Powder River Basin, Wyo.

the first 15 feed coal samples. These element variations result from the variation in the barite, crandallite, and gorceixite mineral content in the different coal samples.

In contrast, analysis of the trace-element content of the feed coal and CCPs at a Kentucky power plant, which utilized coal from several different mines in the Illinois and Appalachian Basins, displayed considerable variability (Affolter and others, 1997). Figure 25 shows such variations for selected elements at that power plant during a 16-month sampling period. These variations reflect the multiple mine sources in two coal

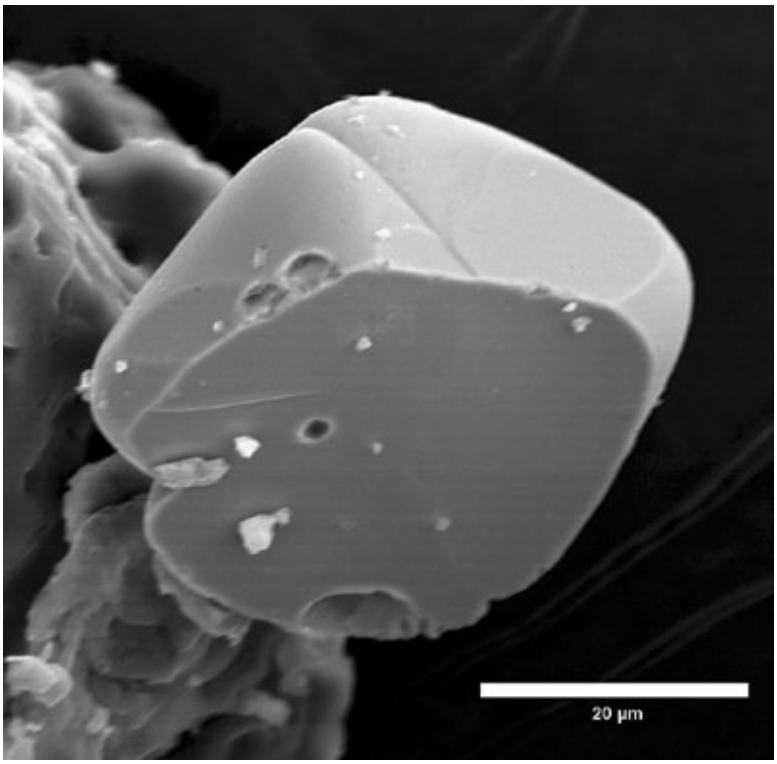

Figure 14. Scanning electron microscope (SEM) secondary electron image of a euhedral crystal of authigenic anatase (TiO_2), from an Indiana power plant feed coal from the Wyodak-Anderson coal zone, Powder River Basin, Wyo.

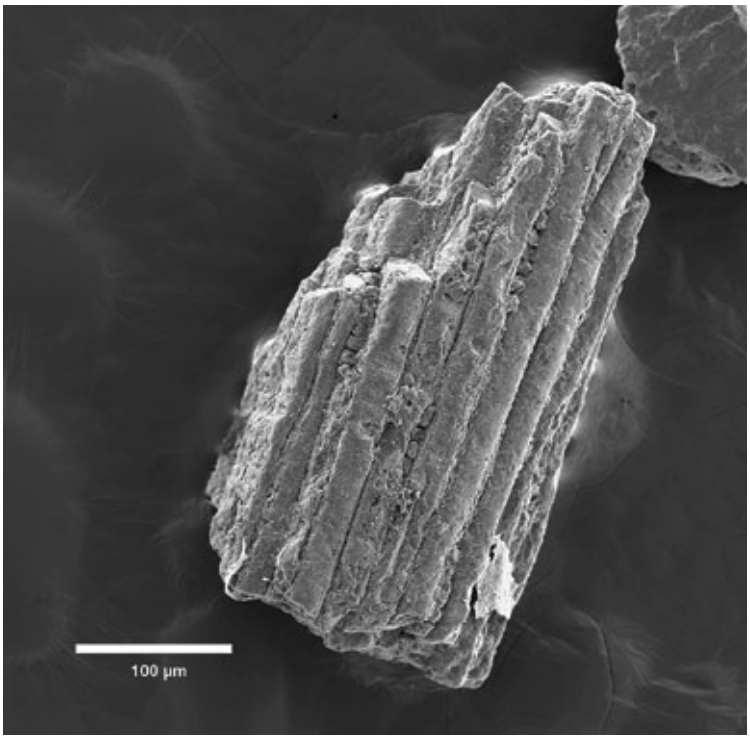

Figure 15. Scanning electron microscope (SEM) secondary electron image of authigenic quartz (SiO_2) that replaced plant matter, from an Indiana power plant feed coal from the Wyodak-Anderson coal zone, Powder River Basin, Wyo.

basins, and the variability in mineral content and amount of the individual phases in the different feed coals.

In general, the trace-element contents in the different fly ashes and bottom ashes collected at the Indiana power plant during the sample period appear to be similar; the composite truck fly ash shows somewhat higher variability and the economizer fly ash slightly lower variability for some elements (Affolter and others, 1999). (Variations in barium and phosphorus contents are shown in figures 23 and 24.) The economizer ash is coarser grained than the truck fly ash: it has a wide range in particle sizes with different adsorption characteristics, whereas the truck fly ash is a composite sample

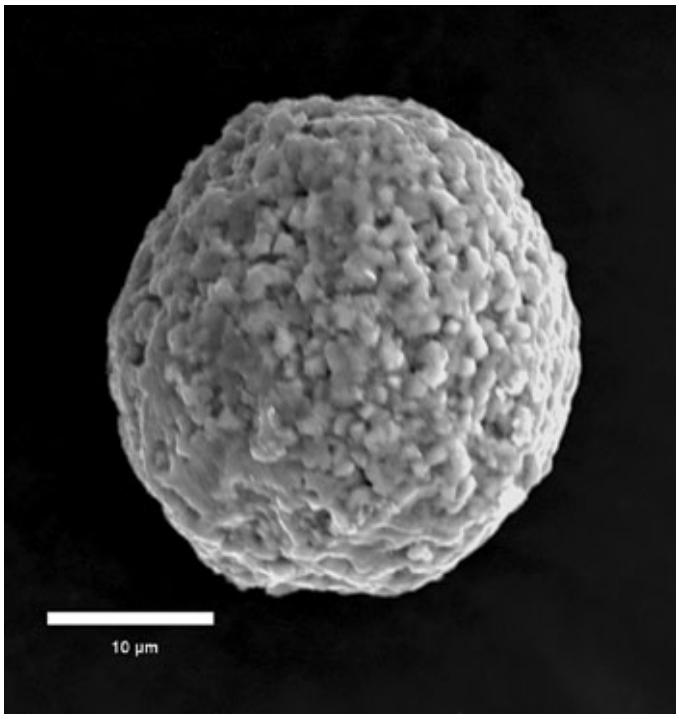

Figure 16. Scanning electron microscope (SEM) secondary electron image of an iron oxide sphere, probably a fecal pellet, from an Indiana power plant feed coal from the Wyodak-Anderson coal zone, Powder River Basin, Wyo.

with adsorption characteristics common to both new and old fly ash samples. This lack of variation in trace-element content is in strong contrast to results from other studies (Affolter and others, 1997) in which feed coal was utilized from numerous sources and showed considerable variation in element chemistry. Because the Indiana power plant utilizes coal from the Wyodak-Anderson coal zone, particle-size distribution and shape of the fly ash grains in the samples collected from old and new automated fly ash samplers are similar. The new fly ash sampler contained greater quantities of very fine particles because of the sampler's funnel shape when compared to the old sampler, which was a pipe shape (Gregory H. Keenan, American Electric Power, written commun., 1999). A more complete discussion of temporal variation of the Wyodak-Anderson feed coal is underway (R.H. Affolter and others, work in progress).

Feed coal samples from the Wyodak-Anderson coal contain higher amounts of Ba, Ca, Mg, Na, Sr, and P than eastern feed coal (Affolter and others, 1997; Brownfield and others, 1997; Brownfield, Affolter, Cathcart, O'Connor, and Brownfield, 1999). These elements are associated with hydrated alumino-phosphate (crandallite and gorceixite) and clay minerals, as well as apatite, biotite, calcite, and barite. Except for calcite, apatite, and biotite, the minerals associated with these elements are derived from dissolution and devitrification of volcanic ash. The original ash probably consisted of silica glass, beta-form quartz phenocrysts, biotite, zircon, potassium feldspar, and plagioclase. Pyroxenes and amphiboles, which are common in volcanic airfall ash and are relatively unstable minerals, were not detected in the coal. Pyroxenes and amphiboles may have been present in the original ash; if so, they were most likely dissolved in the acid environment of the peat-forming mires.

The elemental and minor minerals associations in the Wyodak-Anderson coal samples indicate that the coals contain reworked and (or) altered volcanic ash, based on the presence of (1) clear, sharp angular quartz grains, some of which are blade and flake shaped and may be broken phenocrysts; (2) beta-form quartz (high temperature) phenocrysts; (3) euhedral zircon and biotite crystals; and (4) alumino-phosphate (crandallite and gorceixite) minerals (Brownfield and others, 1987; Triplehorn and others, 1991; Crowley and others, 1993). Dissolution and alteration of the volcanic mineral suite most likely occurred in the early diagenetic peat-forming stage (strong leaching environment) and (or) possibly during the late diagenetic coalification stage, and contributed to the authigenic formation of kaolinite, quartz, calcite, anatase, crandallite, gorceixite, and barite.

Major, minor, and trace elements in coal can occur in three phases: (1) included in, or attached to, organic

Table 4. Concentrations of major and minor oxides for feed coal, fly ash, and bottom ash for the first 15 days of sampling (*n*=15) from an Indiana power plant utilizing coal from the Wyodak-Anderson coal zone, Powder River Basin, Wyo.

[All values are in percent and are presented on an as-determined basis for the feed coal, fly ash and bottom ash; n.d., not determined]

Oxide	Feed coal mean	Fly ash mean	Bottom ash mean
(Ash)	6.1	n.d.	n.d.
SiO_2	23.6	32.3	27.8
Al_2O_3	14.7	18.1	17.5
CaO	20.8	26.4	20.2
MgO	4.9	5.8	4.8
Na_2O	1.6	2.4	1.7
K_2O	.30	.33	.31
Fe_2O_3	5.3	6.5	6.4
TiO_2	1.1	1.4	1.4
P_2O_5	.88	1.0	.81

Table 5. Comparison of concentrations of selected elements of environmental concern for feed coal (*n*=15), fly ash (*n*=25), and bottom ash (*n*=14) from an Indiana power plant utilizing coal from the Wyodak-Anderson coal zone, Powder River Basin, Wyo.

[All values are in parts per million and are presented on an as-determined basis for the feed coal, fly ash, and bottom ash except for Hg and Se, which have been recalculated to an ash basis. Mean ash yield of the feed coal is 6.1 percent]

Element	Feed coal mean	Fly ash mean	Bottom ash mean
As	14	18.7	7.5
Be	3.1	5.1	.81
Cd	.82	.93	.29
Co	27	28	31
Cr	53	62	53
Hg	0.08	.01	0.02
Mn	170	200	200
Ni	32	50	60
Pb	23	38	14
Sb	1.7	2.7	1.1
Se	0.72	29	22
Th	20	30	24
U	6.5	9.4	8.4

compounds as organic complexes or exchangeable cations; (2) in mineral matter as major or trace components of minerals; and (3) only rarely as dissolved constituents of fluids in the coal. Sequential leaching experiments were used to quantify the modes of occurrence of inorganic elements in the feed coal from Wyodak-Anderson coal; results with respect to selected elements are summarized in table 9.

Leaching experiments indicate that at least 40 percent of the Ba, Co, Fe, Mn, P, Pb, Sr, Th, and U is associated with HCl-soluble compounds (table 9), such as carbonates, monosulfides, phosphates, and oxides, whereas at least 50 percent of As, Co, Ni, and Se is associated with insoluble phases or organic matter. About 20 percent of the arsenic is associated with HCl-soluble minerals such as crandallite and gorceixite, where arsenic can substitute for phosphorus or arsenates. Chromium is contained in both clay minerals and organic matter. Beryllium is evenly distributed among silicates (clays, micas, and albite), organic matter, and HCl-soluble compounds such as monazite and beryllium-bearing oxides, hydroxides, or sulfates. Some of the Se, Th, and U is associated with HF- and HNO_3-soluble compounds, including clays and other silicates, as well as pyrite and other disulfides. All of the mercury in the Wyodak-Anderson coal samples appears to be organically associated.

The minerals identified in the feed coal samples contain leachable elements, and these minerals are important modes of occurrence for elements in the Wyodak-Anderson coal. Crandallite and gorceixite (table 3) were found in the feed coal and are aluminum phosphate minerals that can contain Ba, Ca, and Sr. Barite ($BaSO_4$), potassium feldspar, and biotite were also identified in the feed coal and are known to contain trace amounts of barium. HCl-soluble calcite ($CaCO_3$) was detected in trace amounts and is known to contain trace amounts of Ba, Co, Fe, Mn, Ni, Sr, and Pb. Trace amounts of HCl-soluble dolomite ($Ca,Mg(CO_3)_2$), ankerite ($Ca(Fe,Mg,Mn)(CO_3)_2$), siderite ($FeCO_3$), and cerussite ($PbCO_3$) were found in the NaOCl-treated coal samples. Lead can substitute in trace amounts for magnesium in ankerite and dolomite, which may account for the high amounts of lead in the HCl leachate. At least 50 percent of the iron (Fe) is attributed to iron-bearing carbonates, iron oxides (hematite?, fig. 16), iron-bearing silicates (biotite and muscovite); shielded (very small mineral grains surrounded by organic matter) or insoluble minerals (ilmenite), and trace amounts of pyrite account for the remainder.

Palmer and others (1998, 2000) reported selective leaching results for Wyodak-Anderson coal samples and indicated that more than 40 percent of the Co, U, Be, Ca, Fe, Mn, Ba, Zn, Cd, and Pb is associated with HCl-soluble carbonates, iron oxides, or monosulfides, whereas greater than 40 percent of the Al, Cr, and Mo is associated with HF-soluble silicates. Other leaching experiments indicate that more than 40 percent of the As, Cu, Ni, and Sb is associated with acid-insoluble phases and (or) organic matter. Fifty percent or more of the mercury is associated with HNO_3-soluble pyrite or other sulfides. This is in marked contrast to our findings where pyrite was only noted as a trace phase by SEM analysis. Thirty percent of the thorium content was leached by HCl, and another 30 percent was leached by HF.

The abundant Ca-, Mg-, and less abundant P-mineral phases (merrillite, anhydrite, C3A, gehlenite, periclase, lime, perovskite, and whitlockite) in the fly ash and anorthite, augite, and melilite in the bottom ash are from high-temperature alteration of carbonate, clay, alumino-phosphate, biotite, feldspar, and anatase minerals in the feed coal. The feed coal minerals, in part, formed during dissolution and alteration of airfall volcanic ash in the coal (Brownfield, Affolter, Cathcart, and others, 1999). Therefore, the Ca-, Mg-, and P-rich mineral phases in the CCPs are from the high-temperature transformation of volcanic minerals deposited in the peat-forming mire

Table 6. Element concentration data for selected elements from sequential leaching experiments from Wyodak-Anderson coal samples, Powder River Basin, Wyo.

[Original concentrations (ppm, parts per million) are presented on a whole-coal basis; solvent data presented in percent leached by each solvent. Totals can exceed 100 percent because of rounding but are within the expected error of plus or minus 20 percent. id, insufficient data]

Element	As	Ba	Be	Co	Cr	Fe	Hg	Mn	Ni	P	Pb	Se	Sr	Th	U	Zn
Original concentration (ppm)																
Feed coal (RP14)[1]	0.86	240	0.24	1.5	2.8	1,900	0.07	7.4	1.5	230	1.2	0.43	210	1.9	0.39	7.1
Feed coal (RP17)[1]	1.1	330	0.20	2.0	3.6	2,500	0.06	9.8	2.2	260	1.5	0.64	190	1.4	0.45	8.8
Feed coal (RP29)[1]	0.92	320	0.20	1.9	3.6	2,500	0.07	13	2.4	280	1.4	0.36	210	1.2	0.47	7.7
Feed coal average[1]	0.96	300	0.21	1.8	3.3	2,300	0.07	10	2.0	260	1.4	0.48	200	1.5	0.44	7.9
As-mined[2]	0.7	390	0.19	2.5	4.1	2,500	0.07	12.0	4.0	490	1.9	0.3	220	1.1	0.5	16.4
R2[3]	1.2	id	0.40	1.5	6.0	2,500	0.08	8.7	5.1	id	1.6	1.3	id	1.8	0.7	8.1
Percent leached by CH_3COONH_4																
Feed coal	5	10	0	1	1	0	0	10	5	1	0	0	25	0	0	1
As-mined	15	20	0	0	0	0	10	5	0	id	0	id	id	0	0	0
R2	0	id	id	0	0	0	0	10	10	id	id	0	id	5	0	10
Percent leached by HCl																
Feed coal	20	80	35	40	10	40	0	90	20	90	90	0	50	60	60	30
As-mined	10	80	55	40	15	60	0	65	20	id	70	id	id	30	50	55
R2	35	id	id	40	10	60	0	75	10	id	id	5	id	5	25	35
Percent leached by HF																
Feed coal	5	5	30	5	40	10	0	5	5	10	15	0	5	30	30	10
As-mined	10	0	30	20	45	10	5	5	0	id	20	id	id	30	30	5
R2	10	id	id	20	45	10	0	15	15	id	id	0	id	10	50	20
Percent leached by HNO_3																
Feed coal	5	1	1	5	10	1	0	1	5	1	10	30	1	15	5	15
As-mined	15	0	0	10	10	20	50	5	15	id	10	id	id	10	5	15
R2	0	id	id	5	10	20	0	0	10	id	id	5	id	40	5	0
Percent unleached																
Feed coal	65	5	35	50	40	50	100	0	65	1	0	70	20	0	5	45
As-mined	50	0	15	20	30	25	35	20	65	id	0	id	id	30	15	30
R2	55	id	id	35	35	10	100	0	55	id	id	90	id	40	20	35

[1] Feed coal source is Wyodak-Anderson coal zone, Campbell County, Powder River Basin, Wyo., sample collected at power plant (n=3). [2] Sample from Antelope mine, Wyodak-Anderson coal zone, Powder River Basin, Wyo. (n=4) from Palmer and others (2000). [3] Wyodak-Anderson coal sample data (n=4) reported by Palmer and others (2000).

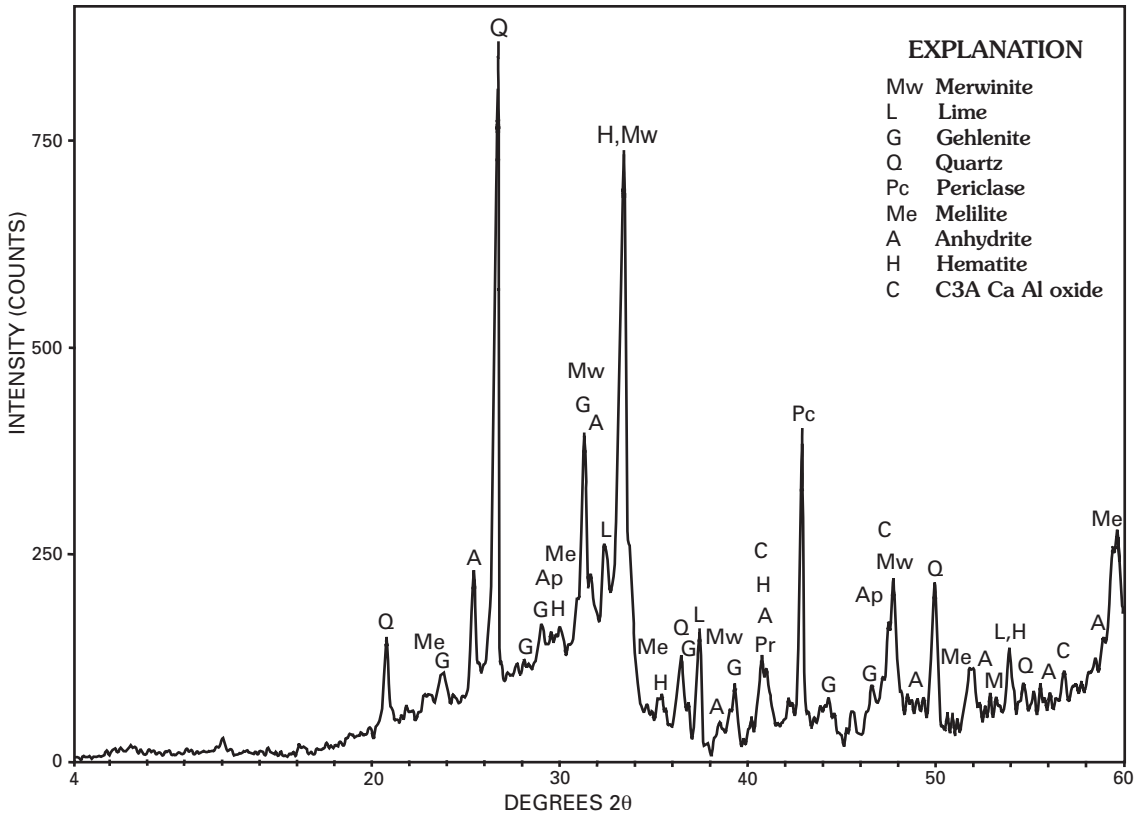

Figure 17. X-ray diffractogram of Class C fly ash from an Indiana power plant burning low-sulfur subbituminous coal from the Wyodak-Anderson coal zone, Powder River Basin, Wyo.

and the authigenic mineral suite derived from the altered volcanic ash. In lower rank coals, major amounts of Ca and Mg may be associated with the organic matter by cation exchange, inasmuch as sequential leaching experiments conducted on feed coal samples indicate that major amounts of Ca and Mg as well as Na are associated with exchangeable cations and organics (table 9). Additionally, detrital mineral input and the epigenetic ground-water flow have affected the final geochemistry of the feed coal.

Two fly ash classes, Class C and Class F, are defined by ASTM (American Society for Testing and Materials, 2003) based on chemical and physical characteristics. Minimum percent of silicon dioxide (SiO_2) plus aluminum oxide (Al_2O_3) plus iron (Fe_2O_3) for Class C fly ash must be at least 70 percent, whereas this sum for Class F fly ash must be at least 50 percent. Class C fly ash is also defined as containing from 15 to 30 percent CaO, with some of the CaO in the form of lime, whereas Class F fly ash CaO content ranges from 1 to 12 percent. Because the feed coal from the Wyodak-Anderson coal zone is rich in Ca (20.8 percent CaO, table 4) the resulting fly ash (26.4 percent CaO, table 4), will be classified as Class C.

The Class C fly ash and bottom ash from the Wyodak-Anderson coal are higher in CaO and MgO and lower in Al_2O_3, Fe_2O_3, and SiO_2 when compared to the eastern United States bituminous Class F fly ash (Brownfield, Affolter, Cathcart, O'Connor, and Brownfield, 1999). The Wyodak-Anderson fly ash contains about 60 percent amorphous calcium-aluminum-silicate glass (table 7), which is highly variable in composition. The associated fly ash- and bottom ash-glass composition is dependent on the rate of quenching and on the amount of substitution by other elements in the glass lattice such as Ca, Fe, K, Mg, and Na. More than 190 fly ash and bottom ash samples (including splits and duplicates) were analyzed by X-ray diffraction (XRD), and the position of the amorphous diffraction (scattering) maxima or glass "hump" was determined. The center point of the scattering maxima reflects the position of the diffraction peak for the crystalline phase that would have exsolved from the incandescent ash had it been allowed to cool slowly. The scattering maxima for the fly ash glass forms an asymmetrical hump centered around 32°–33° 2θ, which is near the major reflection of C3A (fig. 17) and merwinite, whereas the bottom ash glass scattering maxima is centered around 28° 2θ near the major reflection of anorthite (fig. 19). Anorthite (figs. 20, 26), C3A, and merwinite (fig. 27) were identified in analyzed samples. X-ray diffraction analysis of more than 70 eastern fly ash and bottom ash samples resulted in a glass scattering maxima centered around 25°–26° 2θ, which is closer to the position for the major reflection of mullite that is also present

Table 7. Semiquantitative mineralogy of fly-ash samples from an Indiana power plant using feed coal from the Wyodak-Anderson coal zone, Powder River Basin, Wyo., determined by Rietveld X-ray diffraction analysis.

[Values in percent. Due to rounding, total can equal greater than 100 percent; nd, not detected]

Sample No. ---	RP1FAT	RP15FAT	RP22FAT	
Mineral phase				Average
Quartz SiO_2	8.7	6.8	6.7	7.4
Hematite α-Fe_2O_3	2.6	1.5	2.0	2.0
Lime CaO	1.2	0.8	0.6	0.9
Anhydrite $CaSO_4$	3.2	4.3	3.8	3.8
Magnetite $Fe^{2+}Fe_2^{3+}O_4$	nd	0.9	0.5	0.7
Merwinite $Ca_3Mg(SiO_4)_2$	13.6	11.7	7.1	10.8
[1]C3A $Ca_3Al_2O_6$	4.0	4.1	4.2	4.1
Periclase MgO	3.1	2.6	1.8	2.5
Gehlenite $Ca_2Al(Al, Si)O_7$	7.4	10.2	7.8	8.5
Amorphous	56.1	59.2	66.0	60.4
Total	99.9	102.1	100.5	101.1

[1]C3A is a concrete industry abbreviation for a calcium aluminate, $Ca_3Al_2O_6$.

Table 8. Fly ash petrography of selected samples from an Indiana power plant using feed coal from the Wyodak-Anderson coal zone, Powder River Basin, Wyo.

[James C. Hower, written commun., 2001. FAE, economizer fly ash; FAN, new automated fly ash sampler; FAT, silo fly ash sample; FAO, old automated fly ash sampler; t, trace amount. All values in percent]

Sample	Glass	Mullite	Spinel	Quartz	Isotropic coke	Anisotropic coke	Inertinite
RP1- FAE	92.5	4.0	0.5	2.0	0.0	0.0	0.0
RP1- FAN	97.6	1.6	0.8	0.0	0.0	0.0	0.0
RP1- FAT	95.6	1.2	1.2	2.0	0.0	0.0	t
RP4- FAE	91.2	5.6	1.0	2.2	0.0	0.0	0.0
RP4- FAN	95.0	1.4	0.3	3.0	0.0	0.0	t
RP4- FAO	95.0	2.0	0.6	2.4	t	0.0	t
RP4- FAT	97.4	0.2	0.2	2.0	0.0	0.0	0.2
RP14- FAE	88.8	8.6	1.0	1.6	0.0	0.0	0.0
RP14- FAN	95.2	2.2	0.6	2.0	0.0	0.0	t
RP14- FAO	96.8	0.2	0.8	2.0	t	0.0	t
RP14- FAT	97.6	0.2	0.6	1.4	0.0	0.0	0.2
RP17- FAE	90.0	7.6	t	2.4	0.0	0.0	0.0
RP17- FAO	95.8	0.4	1.0	2.6	0.0	0.2	t
RP17-FAT	98.8	0.4	0.2	0.6	t	t	t
RP20-FAE	87.2	8.8	0.8	3.2	0.0	0.0	0.0
RP20-FAO	97.8	t	0.8	1.4	t	0.0	t
RP20-FAT	97.2	0.4	t	2.2	0.0	0.0	0.2
RP29-FAE	86.8	11.2	t	2.0	0.0	0.0	0.0
RP29-FAO	97.6	0.6	0.4	1.4	0.0	t	0.0
RP29-FAT	96.6	0.2	0.4	2.8	0.0	t	0.0

in fly ash samples (Brownfield and others, 1997; Brownfield, Affolter, Cathcart, O'Connor, and Brownfield, 1999). As mullite or aluminum contents decreased, the glass "hump" shifts to a lower 2θ value (22°–24° 2θ), indicating a more siliceous glass. Fly ash from Wyodak-Anderson coal contains more CaO than does bottom ash, 26.4 versus 20.2 percent (table 4), whereas the CaO content in the eastern fly ash and bottom ash ranges from 1.1 to 3.8 percent. Therefore, the scattering maxima appears to reflect differences in chemical composition of fly ash and bottom ash glasses. In Wyodak-Anderson

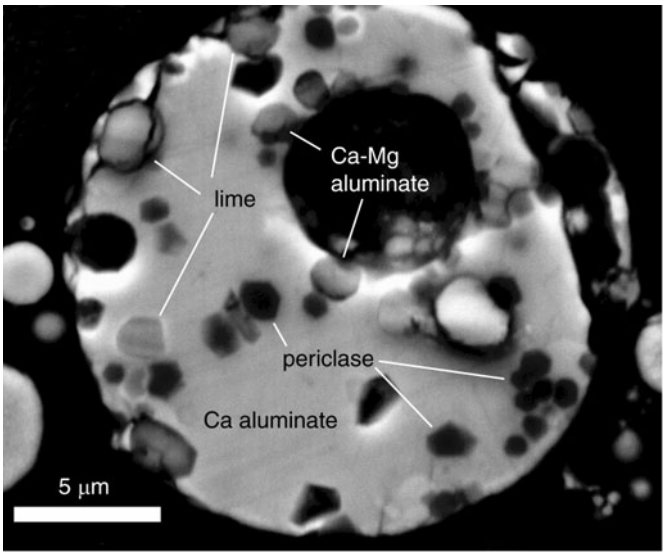

Figure 18. Scanning electron microscope (SEM) backscattered electron image of a fly ash grain with euhedral light-gray lime and dark-gray periclase crystals and subhedral Ca-Mg aluminate crystals in a Ca-aluminate matrix. Sample is from an Indiana power plant fly ash, coal from the Wyodak-Anderson coal zone, Powder River Basin, Wyo.

ashes, the center point of scattering maxima is due to calcium and magnesium content, whereas the glass "hump" of eastern ashes reflects a variation in aluminum content.

Three general chemical types of fly ash (characterized by mineral plus glass assemblages) were noted in the Ca/Mg-rich Wyodak-Anderson fly ash samples examined as part of our overall study by O'Connor and Meeker (1999) using optical petrographic microscope, scanning electron microscope (SEM), electron microprobe analyzer (EPMA), and Gandolfi, bulk-powder, and Rietveld X-ray diffraction techniques. That these characteristic assemblages or types commonly appear with distinctive and easily recognized mineral phases and crystallization patterns nearly eliminates the need for further analysis. These assemblages are as follows: Type 1, (Ca±Mg) +Al (silica (Si) poor) assemblages (figs. 19 and 27); Type 2, (Ca±Mg)+Si (moderate aluminum (Al) content) assemblages (figs. 20, 27, 28); and Type 3, (Ca±Mg)+Si+P (variable Al) assemblages (figs. 29 and 30). In addition to the three major assemblages, minor iron (Fe)-bearing minerals (pyrite, for example) in the feed coal resulted in complex Fe-spinel, ferrite, and Fe-silicate phases being present (figs. 20, 26) in some fly ash grains.

Among the diverse mineral phases identified in our study, oxides, low-Si silicates, and aluminates commonly occur as relatively large (>10 μm) unzoned subhedral to euhedral or graphically intergrown crystals within glass, some of which approach ideal stoichiometry. The crystal morphologies and chemical compositions indicate that mineral growth probably occurred near or at equilibrium with the glass phase.

One of the silica-poor fly ash mineral assemblages, shown in figure 18, consists of euhedral crystals of periclase and euhedral to rounded subhedral crystals of lime observed growing in a matrix of approximately 3:2 Ca aluminate (Type 1; see preceding). Small subhedral crystals of an unknown Ca-Mg-aluminate compound were also noted by energy dispersive spectral (EDS) analysis with a possible $3CaO{\cdot}MgO{\cdot}2Al_2O_3$ composition. Fly ash grains with this composition likely would have exsolved lime and periclase, changing in composition along the liquid stability field of aluminate (O'Connor and Meeker, 1999).

Commonly, the silica-poor assemblages (Type 1) contain euhedral octagons or cubes of periclase and possibly minor melilite (O'Connor and Meeker, 1999), which crystallized in a glass matrix of 3:2 calcium and 12:14 (Ca) aluminate, gehlenite ($Ca_2Al(AlSi)O_7$), or mayenite ($Ca_{12}Al_{14}O_{33}$). Other silica-poor mineral assemblages include bredigite ($Ca_7Mg(SiO_4)_4$, fig. 28) or larnite (β-Ca_2SiO_4) and a 3:2 Ca aluminate (C3A?, $Ca_3Al_2O_6$). Other Type 1 fly ash grains contain melilite ($(Ca,Na)_2(Al,Mg)(Si,Al)_2O_7$) and larnite ($\beta$-$Ca_2SiO_4$) with 3Ca aluminate glass.

Some Si+Al-bearing fly ash grains retain enough element mobility to form nearly stoichiometric crystals. High magnesium content within the fly ash grain apparently aids in the mobility of elements (O'Connor and Meeker, 1999). One such Type 1 grain is shown in figure 27 where euhedral crystals of periclase (MgO) and merwinite ($Ca_2Mg(SiO_4)_2$) exsolved from a glass consisting of 3Ca aluminate.

The increase of silica content in the fly ash grains increases viscosity and interferes with the ability to form well-crystallized minerals in the short time available for crystallization during combustion. Bottom ash samples, however, remain at elevated temperatures for a longer period, and more complete ionic mobility is possible. A bottom ash sample (Type 2; see preceding) showing a coarse intergrowth of plagioclase (anorthite, $CaAl_2Si_2O_8$) and fassaitic pyroxene (ferrian-aluminian diopside, $CaMgSi_2O_6$) or augite $(Ca,Na)(Mg,Fe,Al,Ti)(Si,Al)_2O_6$) is shown in figure 20. The anorthite is relatively pure calcic plagioclase ($An_{96}Ab_4$). The pyroxene has a high aluminum and titanium content and is distinctly compositionally zoned, illustrating the restricted element mobility in the richer silica-glasses.

As much as 5 percent of the fly ash grains examined in our study contains phosphorus or phosphorus-bearing minerals (Type 3; see preceding), representative of the Class 5 type fly ash of O'Connor (1997a). The phosphorus, which was likely derived from apatite ($Ca_5(PO_4)_3$), crandallite group minerals, or amorphous hydrous aluminum silicate material in the feed coal, is responsible for the assemblage of cryptocrystalline phases of which whitlockite ($Ca_9(Mg,Fe)(PO_4)_6(PO_3,OH)$), its anhydrous analog merrillite, and (or) α-$Ca_3(PO_4)_2$ are the probable constituents (O'Connor, 1997b). Figure 29 shows a Type 3 fly ash grain containing euhedral crystals of corundum (Al_2O_3) in a cryptocrystalline phosphate/silicate glass. A rare phosphorus-bearing fly ash grain (Type 3) with rare earth element content is shown in figure 30. The small size of the crystals in the glass precludes meaningful electron microprobe analysis, but a semiquantitative analysis of the

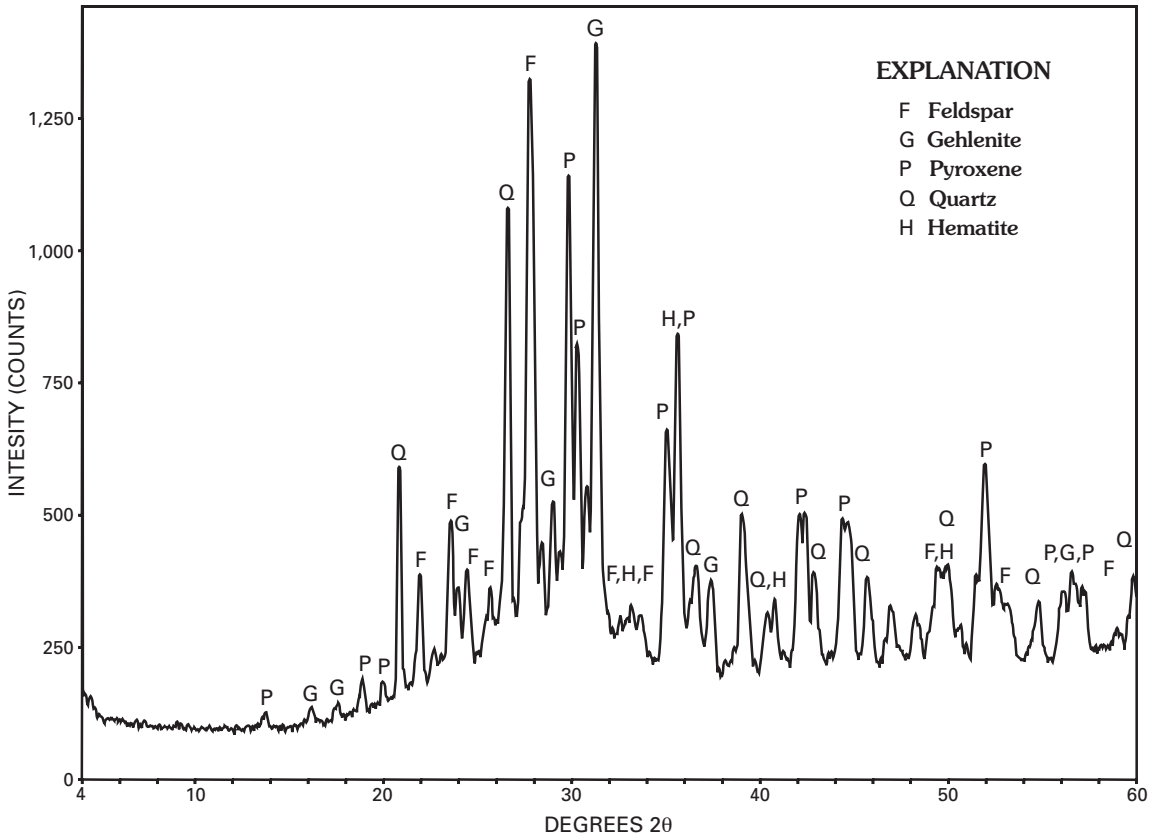

Figure 19. X-ray diffractogram of bottom ash from an Indiana power plant burning feed coal from the Wyodak-Anderson coal zone, Powder River Basin, Wyo.

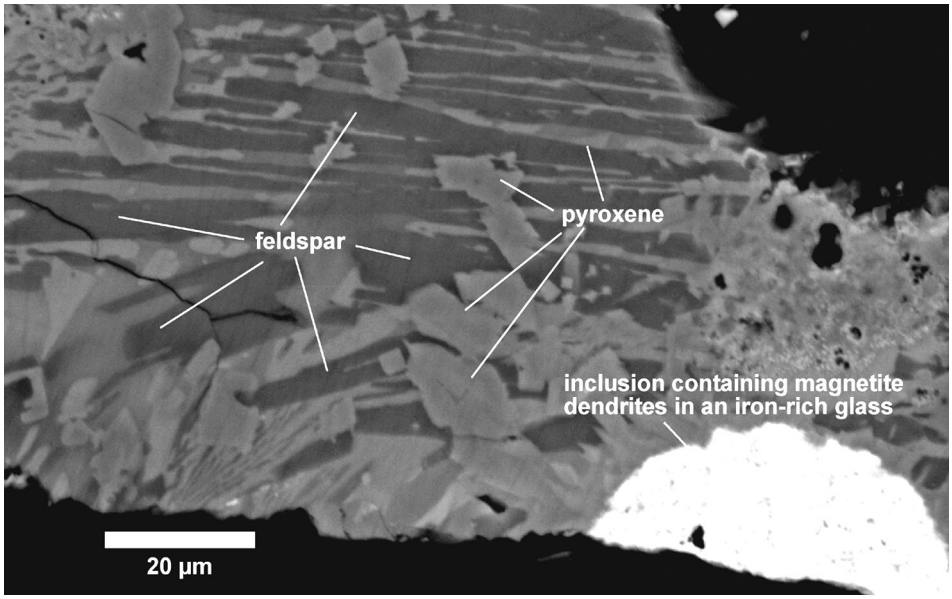

Figure 20. Scanning electron microscope (SEM) backscattered electron image of a (Ca+Mg)-rich bottom ash grain showing coarse intergrowth of feldspar (anorthite?) and pyroxene (fassaite?). Bright inclusion in lower right contains magnetite dendrites (bright white) that exsolved from an iron-rich glass (light gray). Sample is from an Indiana power plant bottom ash, coal from the Wyodak-Anderson coal zone, Powder River Basin, Wyo.

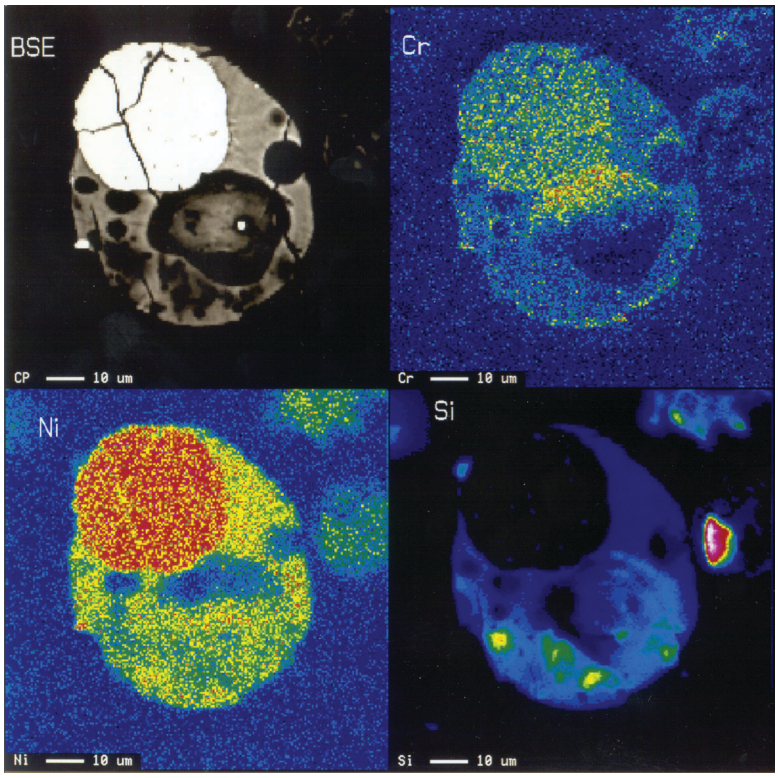

Figure 21. Electron microprobe backscattered electron image (BSE) and element X-ray intensity maps showing relative abundances and distribution of chromium (Cr), nickel (Ni), and silica (Si) in a Kentucky power plant ferrite-rich fly ash grain. Image from Robert B. Finkelman.

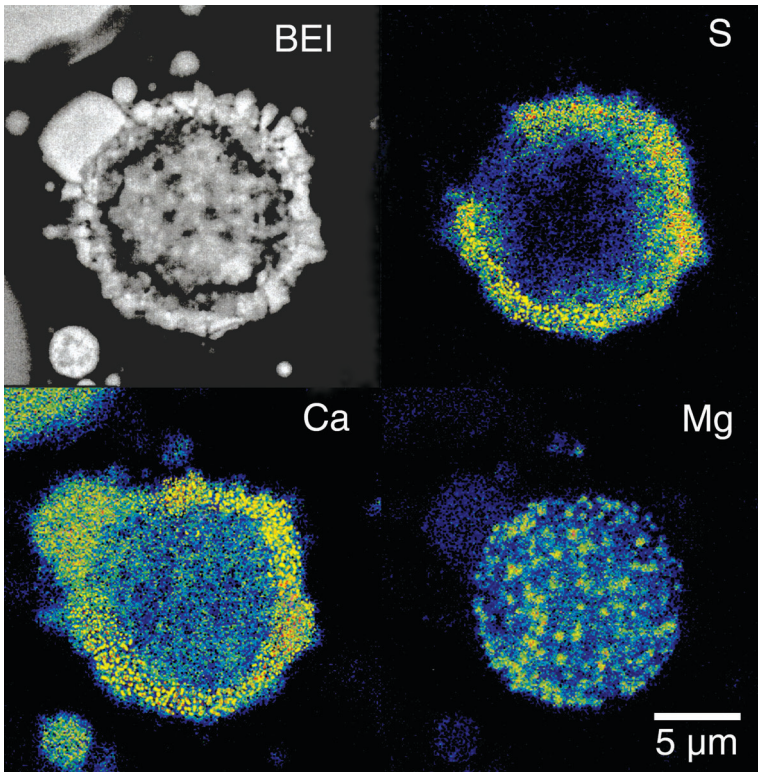

Figure 22. Scanning electron microscope (SEM) backscattered electron image (BEI) showing a bright anhydrite coating and element X-ray intensity maps showing relative abundances and distribution of sulfur (S), calcium (Ca), and magnesium (Mg) in one Indiana power plant fly ash grain. The higher abundances of Ca and S are the result of a thin anhydrite ($CaSO_4$) coating on the fly ash grain. The bright areas in the lower left image are periclase crystals (MgO) in a Ca-aluminate glass. Sample is from an Indiana power plant fly ash, coal from the Wyodak-Anderson coal zone, Powder River Basin, Wyo.

cryptocrystalline material shows a rare earth element content greater than 26 percent, dominated by the heavy rare earth elements. Phosphorus-bearing fly ash grains contain anomalously high uranium, arsenic, and fluorine contents (O'Connor, 1997b). In our study, the rare earth element anomaly was the major variation in the fly ash chemistry detected among the analyzed phosphorus-bearing fly ash grains.

The fly ash grains containing relatively more iron exsolve an iron spinel (fig. 26), generally magnetite and magnesioferrite ($MgFe_2O_3$), with many of the same crystallization features

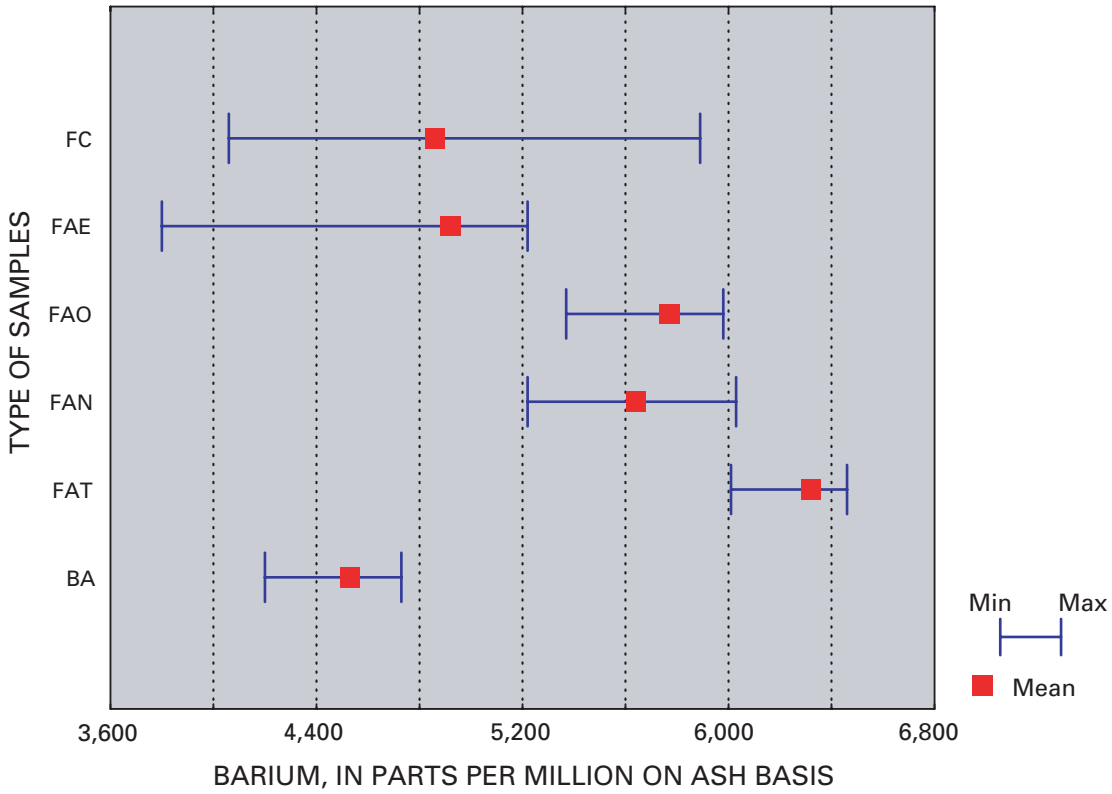

Figure 23. Variation of barium content during the first 15 days of sampling (*n*=15) of the feed coal from the Wyodak-Anderson coal zone, Powder River Basin, Wyo., and combustion products at the Indiana power plant. Range plot shows mean, minimum, and maximum values from feed coal (FC), economizer fly ash (FAE), old fly ash sampler (FAO), new fly ash sampler (FAN), truck fly ash (FAT), and bottom ash (BA) samples.

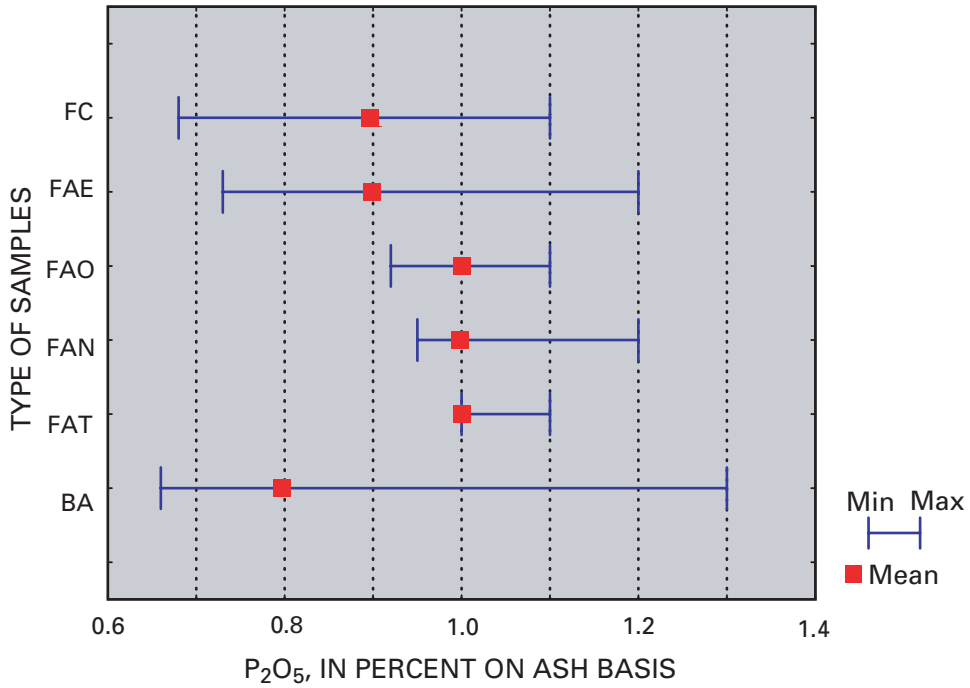

Figure 24. Variation of phosphorus content during the first 15 days of sampling (*n*=15) of the feed coal from the Wyodak-Anderson coal zone, Powder River Basin, Wyo., and combustion products at the Indiana power plant. Range plot shows mean, minimum, and maximum values from feed coal (FC), economizer fly ash (FAE), old fly ash sampler (FAO), new fly ash sampler (FAN), truck fly ash (FAT), and bottom ash (BA) samples.

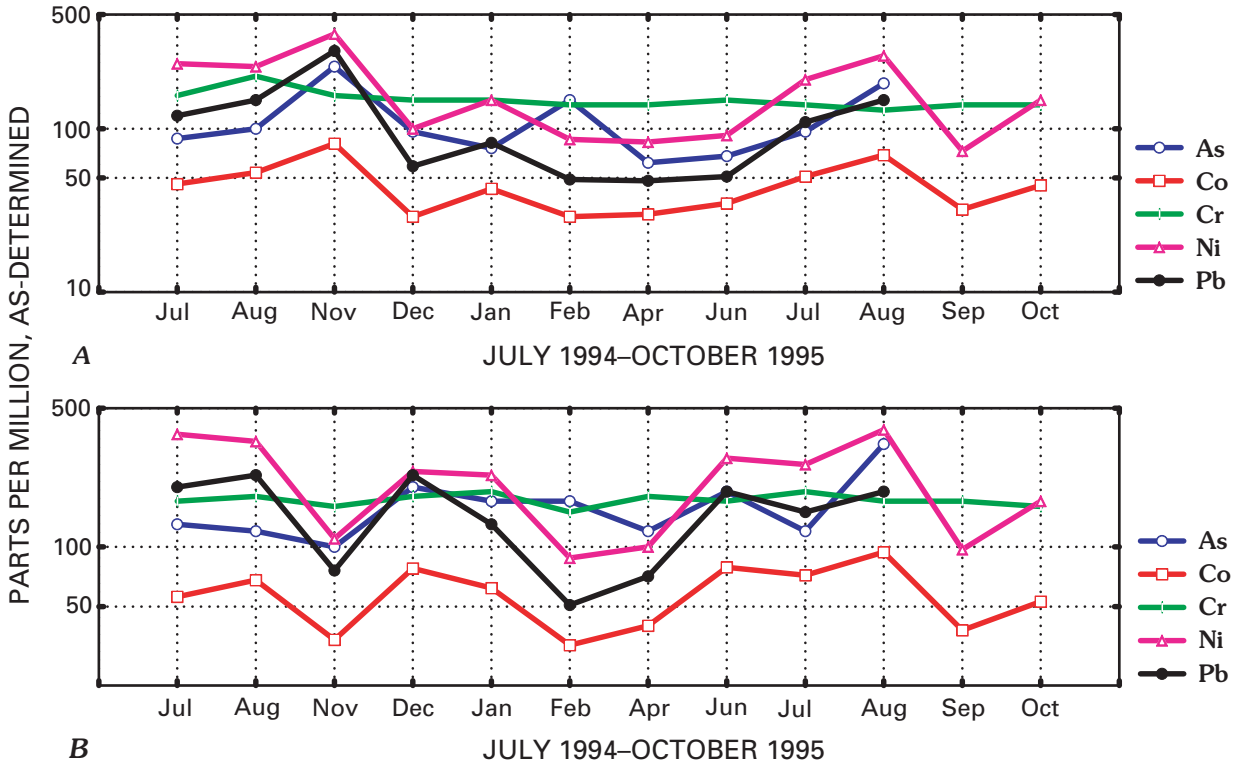

Figure 25. Temporal variation of selected elements in *A*, feed coal, and *B*, fly ash at a Kentucky power plant during 16-month sampling period.

Table 9. Modes of occurrence data for selected elements for feed coal samples from Wyodak-Anderson coal zone, Powder River Basin, Wyo.

[Mode of occurrence data presented in percent leached by each solvent's compounds and (or) mineral associations. NH_4=water-soluble compounds, some carbonates, and elements bonded onto exchangeable sites; HCl=carbonates, iron oxides, monosulfides, phosphates, and chelated organic compounds; HF= silicates; HNO_3= disulfides, especially pyrite. Feed coal source is the Wyodak-Anderson coal (*n*=3), Campbell County, Powder River Basin, Wyo., sample collected at power plant. *indicates an element of environmental interest (U.S. Statutes at Large, 1990). Totals can exceed 100 percent because of rounding but are within the expected error of plus or minus 20 percent]

Element	Exchangeable cations, water-soluble compounds	Pyrite and other disulfides	Silicates	Carbonates, arsenates, iron oxides, monosulfides, phosphates and sulfates	Organic associations or insoluble and shielded minerals
As*	5	5	5	20	65
Ba	10	1	5	80	5
Be*	0	1	30	35	35
Ca	40	1	1	55	5
Co*	1	5	5	40	50
Cr*	1	10	40	10	40
Fe	0	1	10	40	50
Hg*	0	0	0	0	100
Mg	60	0	1	25	15
Mn*	10	1	5	90	0
Na	90	5	2	5	0
Ni*	5	5	5	20	65
P	1	1	10	90	1
Pb	0	10	15	90	0
Se*	0	30	0	0	70
Sr	25	1	5	50	20
Th*	0	15	30	60	0
U*	0	5	30	60	5
Zn	1	15	10	30	45

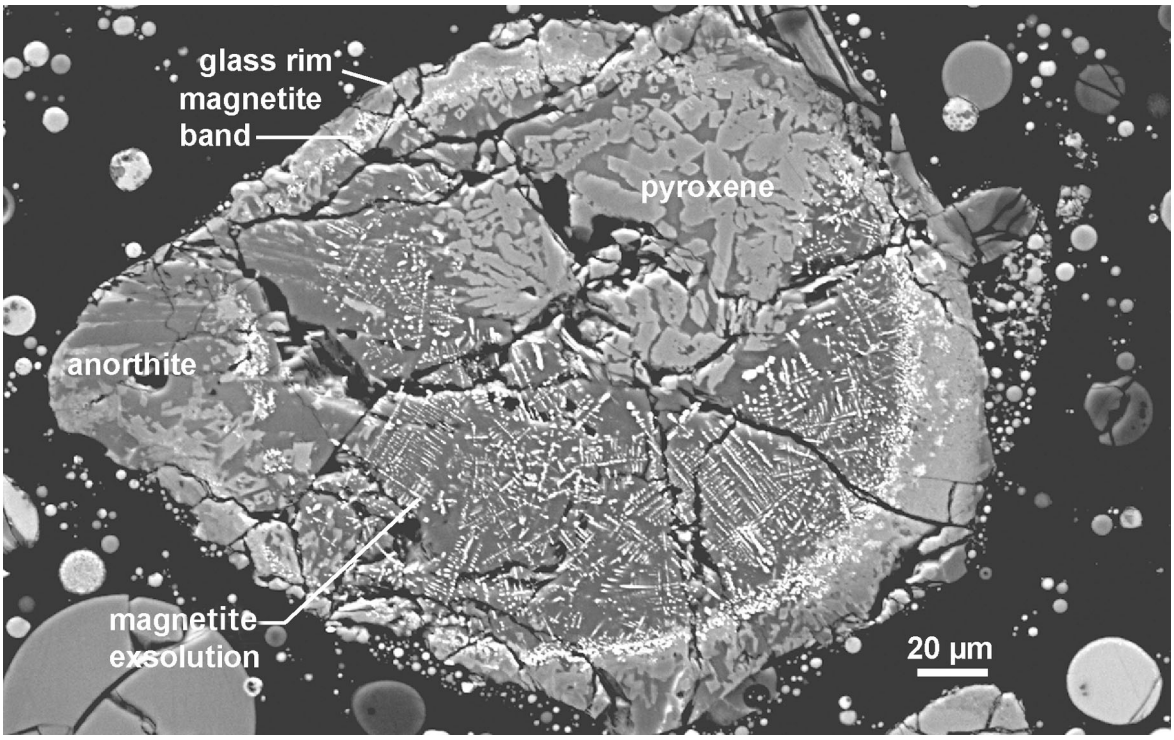

Figure 26. Scanning electron microscope (SEM) backscattered electron image of a (Ca+Mg+Fe+Al+Si)-rich bottom ash grain showing exsolution dendrites of magnetite ($Fe^{2+}Fe_2^{3+}O_4$) in a matrix of anorthite ($CaAl_2Si_2O_6$) and fassaitic pyroxene (ferrian aluminian diopside, $CaMgSi_2O_6$) or augite, $(Ca,Na)(Mg,Fe,Al,Ti)(Si,Al)_2O_6$). Highly variable conditions in the boiler allowed chemical zonation to develop, causing formation of a band of magnetite surrounding the silicate core and a rim of silicate glass with a pyroxene composition. Sample is from an Indiana power plant bottom ash, coal from the Wyodak-Anderson coal zone, Powder River Basin, Wyo.

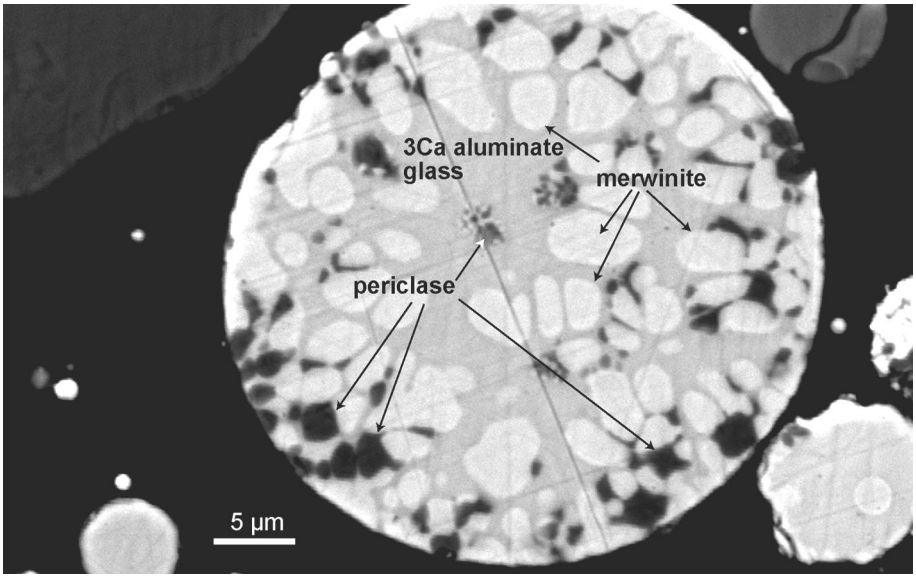

Figure 27. Scanning electron microscope (SEM) backscattered electron image of a Ca+Mg-rich fly ash grain showing euhedral crystals of periclase (MgO) and merwinite ($Ca_3Mg(SiO_4)_2$) in a 3Ca aluminate-silicate glass. Sample is from an Indiana power plant fly ash, coal from the Wyodak-Anderson coal zone, Powder River Basin, Wyo.

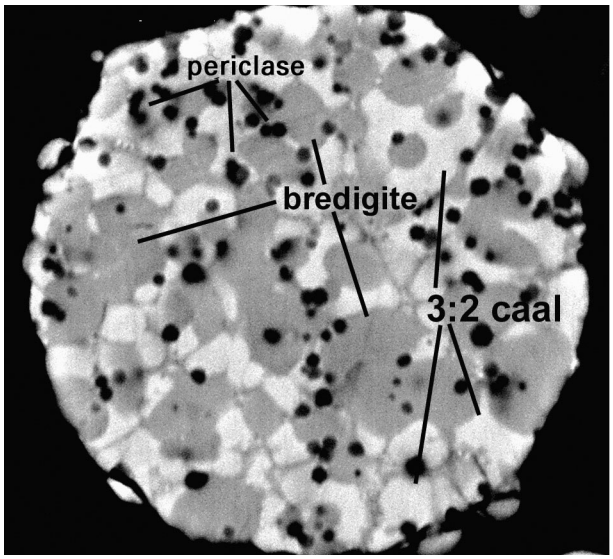

Figure 28. Scanning electron microscope (SEM) backscattered electron image of a (Ca+Mg)-rich fly ash grain showing small dark euhedral periclase (MgO) crystals, subhedral gray crystals of bredigite? (β-Ca_2SiO_4), and bright 3:2 Ca aluminate (3:2 CaAl, C_3A?, $Ca_3Al_2O_6$)). Sample is from an Indiana power plant fly ash, coal from the Wyodak-Anderson coal zone, Powder River Basin, Wyo.

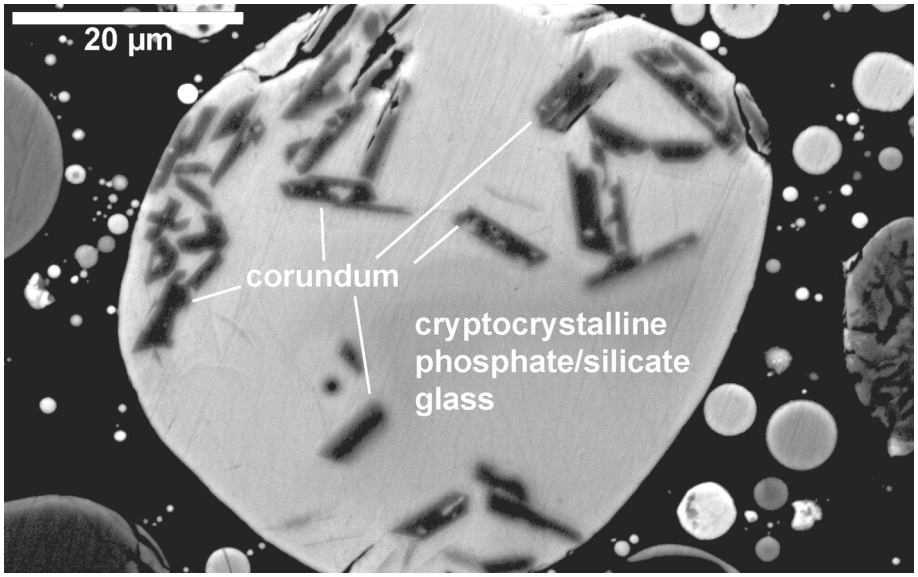

Figure 29. Scanning electron microscope (SEM) backscattered electron image of a (Ca+Si+Al+P)-rich fly ash grain showing euhedral crystals of corundum (Al_2O_3) in a phosphate-silicate glass. Sample is from an Indiana power plant fly ash, coal from the Wyodak-Anderson coal zone, Powder River Basin, Wyo.

noted in fly ash from other eastern feed coals (Brownfield and others, 1997; O'Connor, 1997a).

Anhydrite ($CaSO_4$) was detected in all the fly ash samples by XRD (fig. 17), microprobe, and SEM analyses (element X-ray intensity mapping, fig. 22), forming as a result of the high contents of CaO and the presence of SO_3. The lime (CaO) in the fly ash acted as a self-contained "scrubber" for SO_3, where CaO + SO_3 formed anhydrite during combustion or as a precipitate on fly ash grains in the upper parts of the boiler.

Fly ash is an aluminous and siliceous material that, in the presence of water, will react with the calcium in the lime to produce calcium silicate hydrates with cementitious properties. This is known as a pozzolanic reaction. The Class C fly ash in this study contains free lime (CaO) and has pozzolanic properties.

Amorphous calcium-aluminate glass, anhydrite, and C3A ($Ca_3Al_2O_6$) in the Indiana power plant fly ash can enhance the pozzolanic reactions causing stored or disposed fly ash

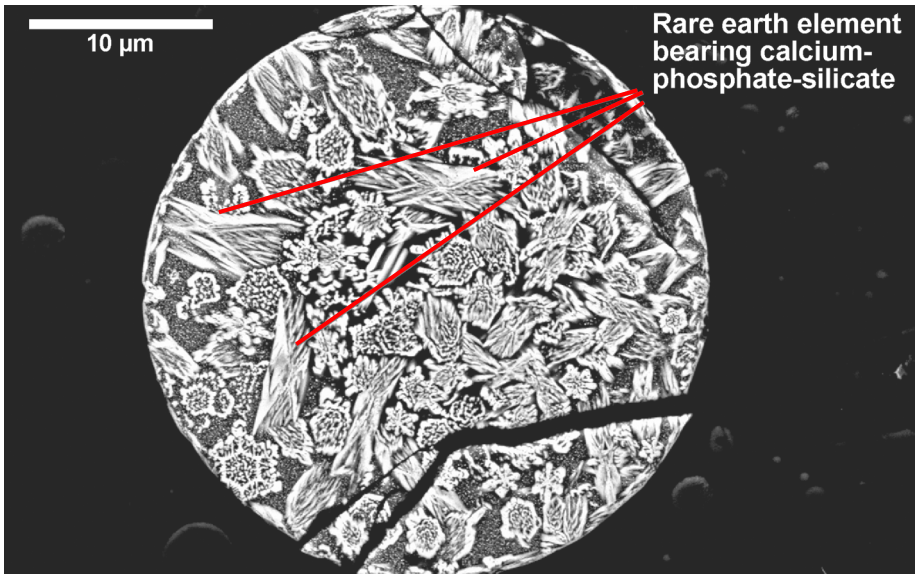

Figure 30. Scanning electron microscope (SEM) backscattered electron image of a rare earth element (REE)-bearing phosphate-silicate fly ash grain. The heavy rare earth elements dominate as determined by semiquantitative, normalized energy dispersive spectral methods. Sample is from an Indiana power plant fly ash, coal from the Wyodak-Anderson coal zone, Powder River Basin, Wyo.

to set-up and harden after contact with water. This enhanced pozzolanic reaction property in Class C fly ashes is known as self-cementing. This reaction forms ettringite and strätlingite in the fly ash at the Indiana power plant disposal site. Analysis of samples from two flow-through column tests by X-ray diffraction revealed a predominance of ettringite, strätlingite, and calcite with a minor amounts of monosulfoaluminate ($Ca_4Al_2(SO_4)(OH)\cdot 10H_2O$) and portlandite ($Ca(OH)_2$). Hydration of the column fly ash formed these secondary minerals, indicating that these minerals can form rapidly. A possible explanation for the absence of portlandite in the disposal site samples is that it may have reacted with atmospheric CO_2 to form calcite. This reaction was also indicated by a long-term leaching study conducted by McCarthy and others (1993) on fly ashes similar to those at the Indiana power plant. Schlorholtz and others (1988) suggested that strätlingite enhances the self-cementing of high-calcium fly ashes, whereas McCarthy and others (1993) believed that ettringite is a strengthening factor in the utilization of high-calcium fly ashes.

Class C fly ashes—with their pozzolanic and self-cementing properties—are widely utilized as raw material in concrete, as a partial replacement (generally by weight) for Portland cement. These fly ashes are also utilized to reduce or stop water drainage at abandoned mine sites, where the fly ash reacts with mine water, causing the fly ash to self-cement, thus reducing or stopping the mine drainage.

Uranium content in the Kentucky and Indiana power plant feed coals is 16 and 8.9 ppm, respectively, and the uranium content of the fly ashes is 19 and 9.0 ppm, respectively. The uranium is organically bound, with lesser amounts associated with uranium-bearing minerals such as apatite, monazite, and zircon. The distribution and form of radioactive elements in fly ash determine the availability of these elements for release to the environment during ash utilization or disposal. The distribution of uranium, as determined by fission-track radiography, was observed to be uniform throughout the glassy grains of the fly ash (figs. 31 and 32). The low amount of surface-bound, potentially leachable uranium suggests that the rate of release of uranium will be slow and controlled by the very slow rate at which the ash grains dissolve (Zielinski and Finkelman, 1997).

Other elements of environmental concern detected by chemical analysis of the Wyodak-Anderson fly ash were difficult to characterize because the elemental contents in fly ash particles were at or below the detection limit of the microbeam instruments. Arsenic is present in larger amounts in the fly ash than in the bottom ash (table 5), and it is uniformly distributed in the Ca-P and glassy fly ash grains when observed by SEM energy dispersive X-ray analysis. Contents of Co, Cr, and Ni are generally similar in both fly ash and bottom ash, and are enriched in the magnetic fraction. Magnetite and magnesioferrite may contain trace amounts of Co, Cr, and Ni. Contents of Sb, Be, Pb, and Se are greater in fly ash compared to bottom ash, and leaching data indicate that these elements were most likely volatilized (table 9) during combustion and are distributed throughout the glassy grains.

Coal and coal combustion products (CCPs) can alter the composition of aqueous solutions through water-rock interactions. These water-rock interactions can be an important environmental consideration in the use of coal for energy production, especially because CCPs can be used in building materials and as soil amendments, and also are disposed

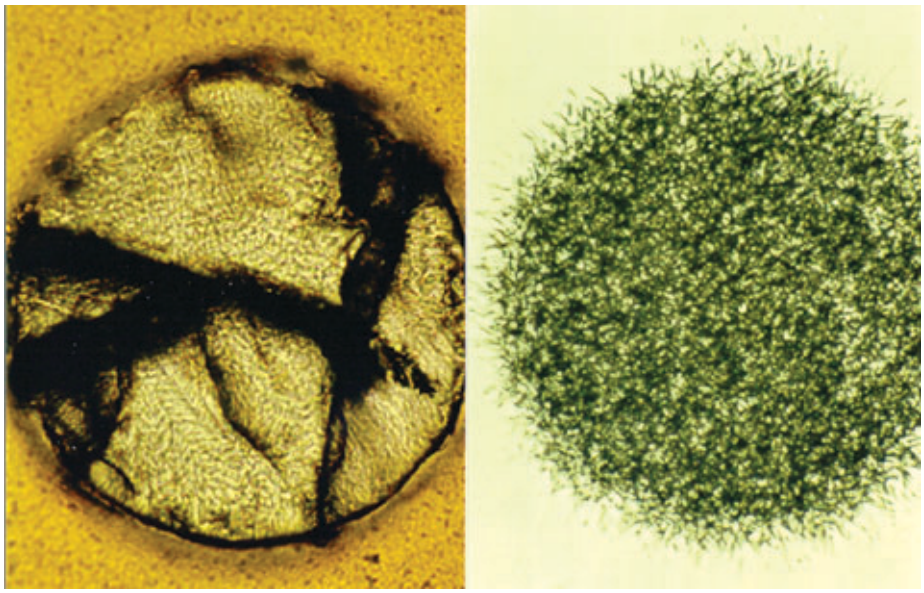

Figure 31. Photograph (left) of a Ca-P rich fly ash grain and its fission track radiograph (right). Uranium distribution and concentration are indicated by the location and density of the fission tracks in the radiograph. Size of photograph and radiograph is approximately 0.25 by 0.15 millimeters. Photograph and radiograph by Robert A. Zielinski. Sample is from an Indiana power plant fly ash, coal from the Wyodak-Anderson coal zone, Powder River Basin, Wyo.

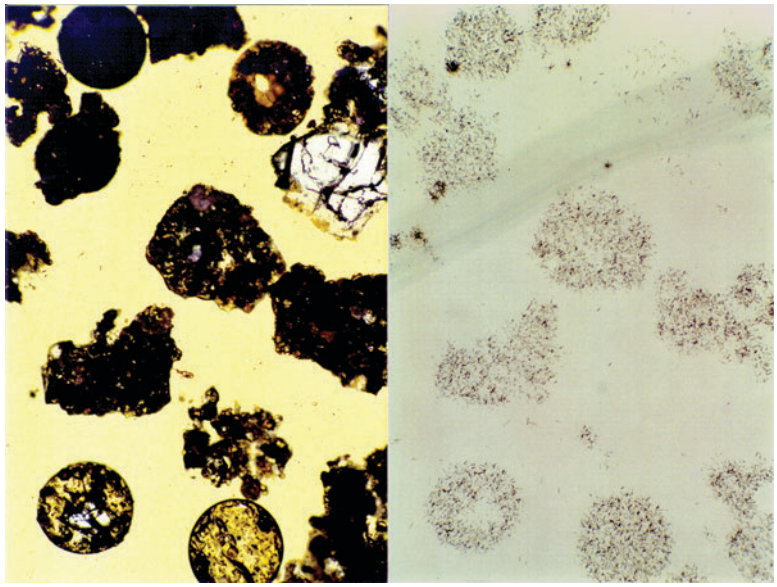

Figure 32. Photograph (left) of fly ash grains with mineral inclusions and its fission track radiograph (right). Uranium distribution and concentration are indicated by the location and density of the fission tracks in the radiograph. Bright mineral inclusions are quartz and contain very low concentrations of uranium. Size of photograph and radiograph is approximately 1.0 by 0.6 millimeters. Photograph and radiograph by Robert A. Zielinski. Sample is from an Indiana power plant fly ash, coal from the Wyodak-Anderson coal zone, Powder River Basin, Wyo.

in surface impoundments. The water-rock interactions can be determined by laboratory techniques that allow mixing of solids and leaching solutions that simulate environmental conditions where leachable metals may be mobilized from the disposal or utilization of fly ash.

Column tests are used to determine long-term (days to months) leaching behaviors of fly ash, simulating the flow of ground or surface water through a material in the natural environment. Figure 33 shows one example in which the percentage of arsenic leached from the Wyodak-Anderson fly ash (24.9 ppm initial As) was relatively small, whereas the cumulative amount of arsenic leached from the fly ash was small—but still increasing—after 70 days. Only about 1.1 percent of the initial arsenic (or 0.27 ppm As) was leached from the fly ash after 70 days. Another example (fig. 34) shows the percentage of arsenic leached from the Kentucky plant fly ash (40 ppm initial As) in 18-hour batch tests to have been relatively small, but the cumulative amount of arsenic leached from the fly ash was significant during a column test. In the Kentucky fly ash, the amount of arsenic being leached seemed to be decreasing during the later part of the column test, although the total amount of arsenic leached from the fly ash was nearly 25 percent or 10 ppm in 64 days (Rice and others, 1999).

Reactions between the solid phase, such as fly ash, and the solution caused a change in the solution composition, which affects the pH and the mobility of trace elements. For fly ash, the original composition of the feed coal, mineral composition, the size of the fly ash particles, and the combustion conditions influence the extent to which trace metals are leached from the fly ash and substantially change solution composition. As an example, figure 35 shows pH and concentration of five selected elements in a solution of deionized

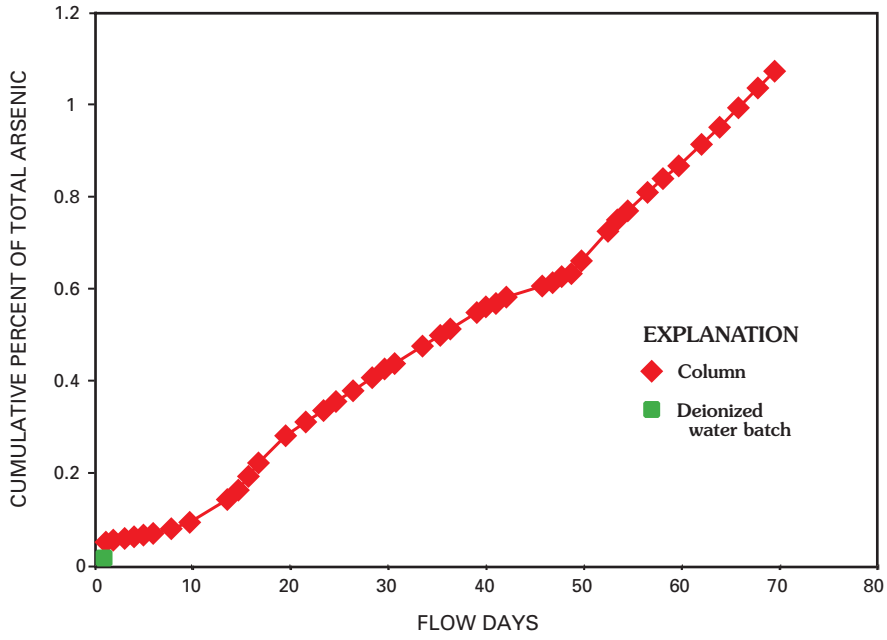

Figure 33. Percentage of arsenic (As) leached from an Indiana power plant fly ash (24.9 ppm initial As) by deionized water in a flow-through column test compared to the percentage leached by an 18-hour batch test (0.02 percent leached) using deionized water. Sample is from an Indiana power plant fly ash, coal from the Wyodak-Anderson coal zone, Powder River Basin, Wyo.

water in contact with the Wyodak-Anderson fly ash. The pH of the solution is initially acidic (pH=5.5) from the deionized water, and the trace metals have relatively low concentrations in solution. Almost instantly, lime (CaO) in the fly ash reacts with the solution, causing a rise in the pH, slowing the mobilization of the elements, especially Al, Fe, and Cu. A second example, figure 36, shows the pH and concentration of the same elements in a solution of deionized water in contact with a fly ash from a Kentucky power plant utilizing a high-sulfur feed coal. The pH of the solution is initially acidic (pH<4), and most of the trace metals have high concentrations in solution because of the rapid dissolution of a sulfate (steklite, $KAl(SO_4)_2$) surface coating (fig. 37) on the fly ash grains (Rice and others, 1999; Fishman and others, 1999). After a few minutes, however, the reaction between lime in the fly ash and the solution begins to raise the pH but at a slower rate because of the lesser amounts of lime present in the Kentucky fly ash. Secondary phases (Al and Fe oxyhydroxides) form from the pH increase resulting in the co-precipitation of some trace metals (for example, Fe, Zn, Cu; fig. 36), which lowers their concentrations. In contrast, the concentration of molybdenum (Mo) increases as the pH increases (fig. 36). The pH dependency of trace metal mobility in batch experiments emphasizes the importance of solution-solid phase interaction studies. A more comprehensive discussion of leaching experiments on the Wyodak-Anderson fly ash is underway (C.A. Rice and others, work in progress).

Leaching experiments range in duration and severity of chemical treatment. Batch leaching tests combine a solution and a fly ash or coal for a selected period of time (seconds to minutes). Several solution compositions may be used sequentially in these batch tests to dissolve different solid phases. Solution compositions of batch tests represent the initial, and commonly highest, concentrations of elements expected to be leached from a material and are used for regulatory purposes in tests such as the U.S. Environmental Protection Agency's toxicity characteristic leaching protocol (TCLP, example, fig. 34).

Summary

Many factors influence feed coal reactions during combustion to form fly ash and bottom ash. Particle size, coal rank, ash content, coal mineralogy, and the trace element composition are important variables that control the combustion of coal-forming gaseous and solid combustion products. Original composition of the feed coal, the combustion conditions, the size of the fly ash particles, and the fly ash mineralogy influence the distribution and mobility of trace metals in fly ash.

Feed coal from the Wyodak-Anderson coal zone studied displayed little variation in element content despite coming from several different mines in Campbell County, Wyo.; small variations are to be expected, however, because of both vertical and lateral changes in mineral content and the amount of individual mineral phases within the coal bed from place to place. The subbituminous Wyodak-Anderson coal has higher Ba, Ca, Mg, Na, Sr, and P contents when compared to eastern bituminous feed coal. Higher contents of these elements are due to the presence of hydrated alumino-phosphates, clays, carbonates, apatite, biotite, and barite. The elemental content and mineral composition of the Wyodak-Anderson coal are indicative of coals having a large influx of volcanic ash.

Analytical analyses using multiple methods indicate that 40 percent or more of Co, Mn, Th, and U contents are from carbonates, phosphates, and oxides, whereas 50 percent or

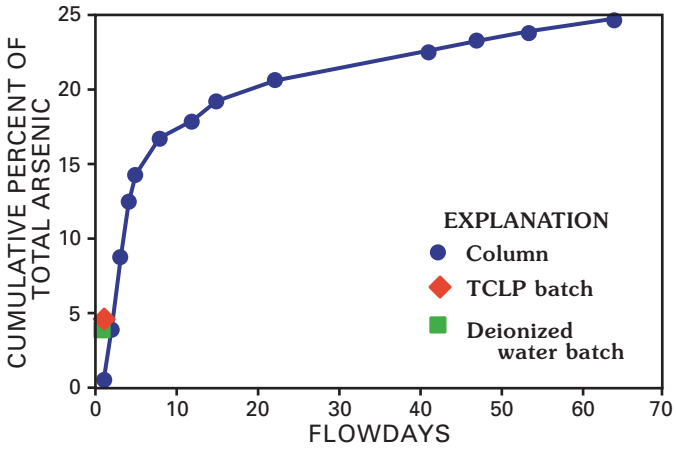

Figure 34. Percentage of arsenic (As) leached from a Kentucky power plant fly ash (40 ppm initial As) by deionized water in a flow-through column test compared to the percentage leached by two 18-hour batch tests. TCLP, U.S. Environmental Protection Agency's toxicity characteristic leaching protocol.

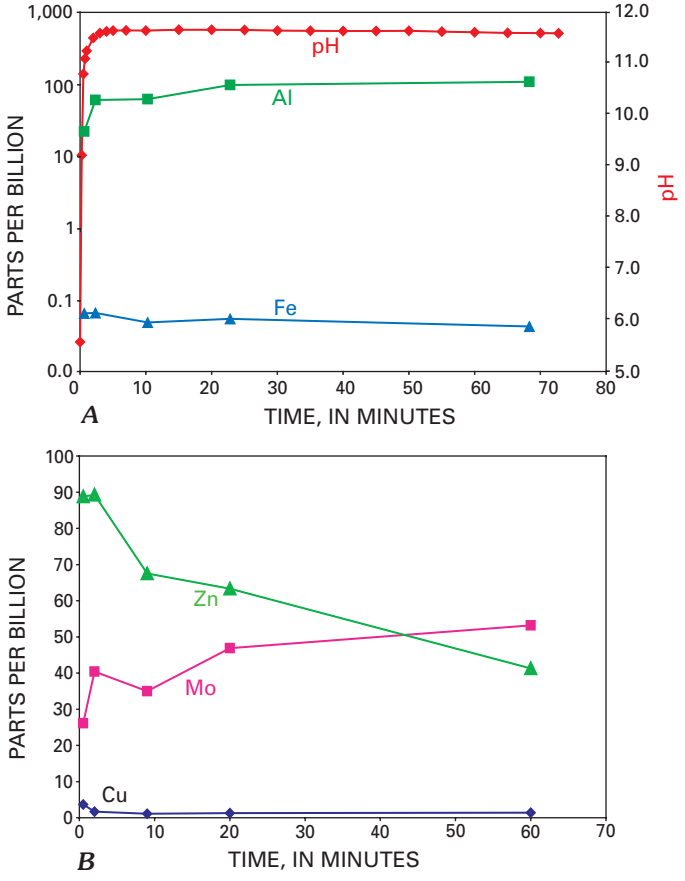

Figure 35. Leachate concentration of *A*, aluminum (Al), iron (Fe), and pH; and *B*, copper (Cu), molybdenum (Mo), and zinc (Zn) during the leaching of a power plant fly ash with deionized water. Sample is from an Indiana power plant fly ash, coal from the Wyodak-Anderson coal zone, Powder River Basin, Wyo.

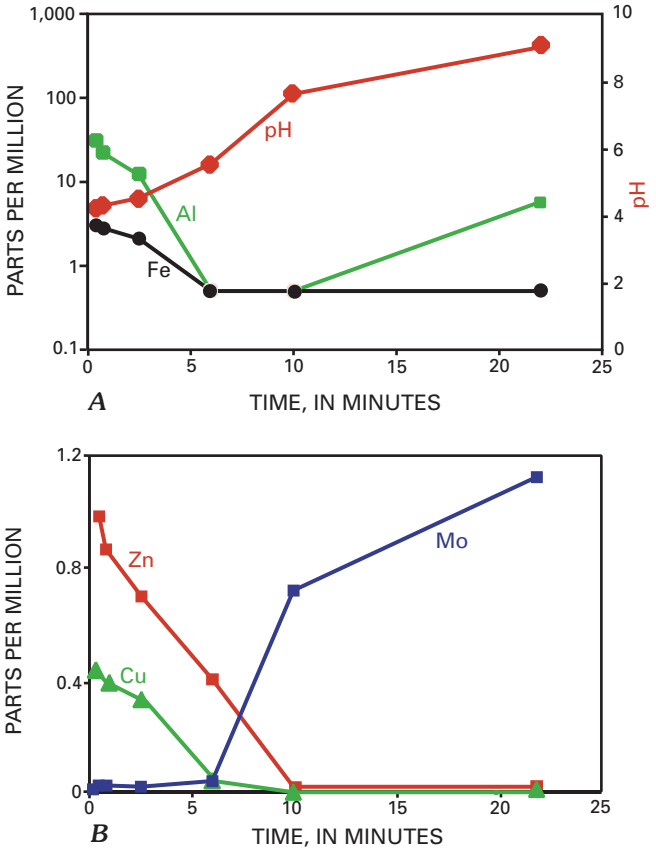

Figure 36. Leachate concentration of *A*, aluminum (Al), iron (Fe), and pH; and *B*, copper (Cu), molybdenum (Mo), and zinc (Zn) during the leaching of a Kentucky power plant fly ash with deionized water.

more of As, Co, Ni, and Se contents are related to organic matter. About 20 percent of the arsenic is associated with arsenates or has substituted for phosphorus in crandallite or gorceixite. Chromium is evenly distributed among the phyllosilicates (clay minerals) and organic matter whereas beryllium is equally shared among the silicates (clays, micas, and albite), organic matter, and unidentified Be-bearing oxides, hydroxides, or sulfates. Portions of the Se, Th, and U are in clays, other silicates, and pyrite. All of the mercury in the Wyodak-Anderson coal samples appears to be associated with organic matter.

Ca- and Mg-rich mineral phases in the Wyodak-Anderson fly and bottom ashes can be attributed to volcanic minerals deposited in the peat-forming mires and their influence on the authigenic mineral suite in the coal. Spinel-ferrite minerals present in the fly ash are related to the presence of Fe-bearing pyroxenes, carbonates, clays, biotite, and pyrite found in the feed coal.

On the basis of XRD analysis, the amorphous diffraction scattering maxima, or glass "hump," appears to reflect differences in chemical composition of fly ash and bottom ash

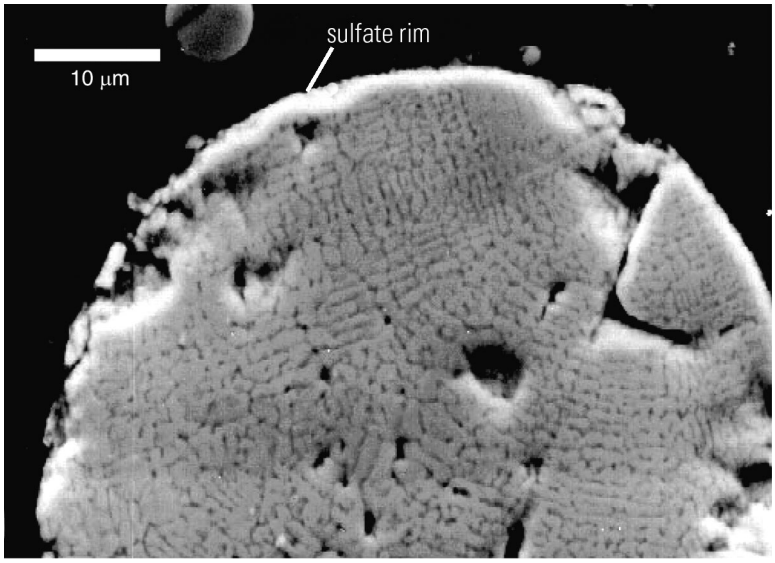

Figure 37. Scanning electron microscope (SEM) backscattered electron image of a spinel-rich Kentucky power plant fly ash grain with a sulfate (steklite, $KAl(SO_4)_2$) enriched coating, which probably controls initial pH (<4) and leaching of some trace metals—see figure 35.

glasses. In Wyodak-Anderson fly and bottom ashes, the center point of scattering maxima is due to calcium and magnesium content, whereas the glass "hump" of eastern fly ash reflects variation in aluminum content.

Wyodak-Anderson Class C fly ash and bottom ash are higher in CaO and MgO and lower in Al_2O_3 and SiO_2 when compared to the eastern United States bituminous Class F fly ash and bottom ash. The scattering maxima related to glass in the Class C fly ash and bottom ash reflect variable calcium and magnesium content, whereas the eastern Class F fly ash and bottom ash glass reflect low calcium and variable aluminum content.

Free lime (CaO) in the fly ash acts as a self-contained "scrubber" for SO_3, forming anhydrite coatings on the fly ash grains either during combustion or as a precipitate before the electrostatic fly-ash collectors. Anhydrite, C3A, and Ca-aluminate glass enhance the self-pozzolanic reactions in the fly ash, causing the fly ash to set up after contact with water-forming ettringite, strätlingite, and calcite. X-ray diffraction analysis of fly ash samples from column tests identified ettringite, strätlingite, monosulfoaluminate, and portlandite, indicating rapid formation during disposal. The lack of portlandite in disposal site samples reflects a reaction of portlandite with atmospheric CO_2, forming calcite.

Arsenic leached from the Wyodak-Anderson fly ash (24.9 ppm initial As) during an 18-hour batch test is minor (0.02 percent leached), whereas the cumulative amount of arsenic leached from the fly ash, although initially small, increased slightly after 70 days to about 1.1 percent (0.27 ppm) of the initial arsenic.

A reaction between lime in the fly ash and water causes a rapid rise in the pH, slowing the mobilization of elements. Considering the high lime content and the resulting hydration of the fly ash, there is little evidence that major amounts of leachable metals are mobilized from the disposal or utilization of Wyodak-Anderson fly ash.

References Cited

Affolter, R.H., and Brownfield, M.E., 1987, Characterization of Lower Williams Fork Formation coals from the eastern Yampa coal field, Routt County, Colorado: Geological Society of America Abstracts with Programs, v. 19, no. 7, p. 567.

Affolter, R.H., Brownfield, M.E., and Breit, G.N., 1997, Temporal variations in the chemistry of feed coal, fly ash, and bottom ash from a coal-fired power plant: Proceedings of the 1997 International Ash Utilization Symposium, Center for Applied Energy Research, Lexington, Ky., October 20–22, 1997, p. 757–764.

Affolter, R.H., Brownfield, M.E., and Cathcart, J.D., 1999, Chemical variation of feed coal and coal combustion products from an Indiana power plant utilizing low sulfur Powder River Basin coal: Proceedings of the 1999 International Ash Utilization Symposium, Center for Applied Energy Research, Lexington, Ky., 7 p. On CD-ROM.

American Society for Testing and Materials (ASTM), 1999a, 1999 Annual Book of ASTM Standards; Petroleum products, lubricants, and fossil fuels, sect. 5, v. 05.05—Gaseous fuels, coal, and coke: Philadelphia, Pa., ASTM, 522 p.

American Society for Testing and Materials (ASTM), 1999b, Standard classification of coals by rank, D388-98a, *in* 1999 Annual Book of ASTM Standards; Petroleum products, lubricants, and fossil fuels, sect. 5, v.05.05—Gaseous fuels, coal, and coke: Philadelphia, Pa., ASTM, p. 188–193.

American Society for Testing and Materials (ASTM), 1999c, Standard practice for preparing coal samples for microscopical analysis by reflected light, D2797-85, *in* 1999 Annual Book of ASTM Standards; Petroleum products, lubricants, and fossil fuels, sect. 5, v. 05.05—Gaseous fuels, coal, and coke: Philadelphia, Pa., ASTM, p. 295–298.

American Society for Testing and Materials (ASTM), 1999d, Standard test method for microscopical determination of the reflectance of vitrinite in a polished specimen of coal, D2798-97, *in* 1999 Annual Book of ASTM Standards; Petroleum products, lubricants, and fossil fuels, sect. 5, v. 05.05—Gaseous fuels, coal, and coke: Philadelphia, Pa., ASTM, p. 299–303.

American Society for Testing and Materials (ASTM), 1999e, Standard test method for microscopical determination of volume percent of physical components of coal, D2799-98a, *in* 1999 Annual Book of ASTM Standards; Petroleum products, lubricants, and fossil fuels, sect. 5, v. 05.05—Gaseous fuels, coal, and coke: Philadelphia, Pa., ASTM, p. 304–307.

American Society for Testing and Materials (ASTM), 2003, Standard specifications for fly ash and raw or calcined natural pozzolan for use as mineral admixture in portland cement concrete, C618-03, *in* 2003 Annual Book of ASTM Standards; Construction, sect. 4, v. 04.02—Concrete and aggregates: Philadelphia, Pa., ASTM, 3 p.

Anderson, J.U., 1963, An improved pretreatment for mineralogical analysis of samples containing organic matter: Clays and Clay Minerals, v. 10, p. 380–388.

Breit, G.N., Finkelman, R.B., Eble, C., Affolter, R.H., Belkin, H.E., Brownfield, M.E., Cathcart, J.D., Crowley, S.S., Hower, J.C., Leventhal, J.S., McGee, J., Palmer, C.A., Reynolds, R.L., Rice, C.A., and Zielinski, R.A., 1996, Systematic investigation of the compositional variations in solid coal combustion waste products: 13th Annual Pittsburgh Coal Conference Proceedings, Pittsburgh, Pa., September 3–7, 1996, p. 1356–1361.

Brindley, G.W., 1945, The effect of grain or particle size on X-ray reflections from mixed powders and alloys considered in relation to the quantitative determination of crystalline substances by X-ray methods: Philosophical Magazine, v. 36, p. 347–369.

Brownfield, M.E., and Affolter, R.H., 1988, Characterization of coals in the lower part of the Williams Fork Formation, Twentymile Park district, eastern Yampa coal field, Routt County, Colorado, *in* Carter, L.M.H., ed., U.S. Geological Survey Research on Energy Resources—1988, Program and Abstracts (V.E. McKelvey Forum on Mineral and Energy Resources): U.S. Geological Survey Circular 1025, p. 6.

Brownfield, M.E., Affolter, R.H., Cathcart, J.D., Brownfield, I.K., Hower, J.C., and Stricker, G.D., 1999, Dispersed volcanic ash in feed coal and its influence on coal combustion products: Proceedings of the 1999 International Ash Utilization Symposium, Center for Applied Energy Research, Lexington, Kentucky, 8 p. On CD-ROM.

Brownfield, M.E., Affolter, R.H., Cathcart, J.D., O'Connor, J.T., and Brownfield, I.K., 1999, Characterization of feed coal and coal combustion products from power plants in Indiana and Kentucky: Proceedings Volume of the 24th International Technical Conference on Coal Utilization and Fuel Systems, Clearwater, Fla., March 8–11, 1999, p. 989–1000.

Brownfield, M.E., Affolter, R.H., and Stricker, G.D., 1987, Crandallite group minerals in the Caps and Q coal beds, Tyonek Formation, Beluga Energy Resource Area, upper Cook Inlet, south-central Alaska, *in* Rao, P.D., ed., Proceedings Focus on Alaska's coal '86: Fairbanks, Alaska, University of Alaska, MIRL Report No. 72, p. 142–149.

Brownfield, M.E., Affolter, R.H., Stricker, G.D., and Hildebrand, R.T., 1995, High chromium contents in Tertiary coal deposits of northwestern Washington—A key to their depositional history: International Journal of Coal Geology, v. 27, p. 153–169.

Brownfield, M.E., Cathcart, J.D., and Affolter, R.H., 1997, Characterization of feed coals and waste products from a coal-burning power plant in Kentucky: Proceedings Volume of 1997 International Ash Utilization Symposium, Lexington, Ky., October 20–22, 1997, p. 780–784.

Cathcart, J.D., Reynolds, R.L., Brownfield, M.E., and Hower, J.C., 1997, Chemical, mineralogical, and magnetic characterization of sized fly ash from a coal-fired power plant in Kentucky: Proceedings of the 1997 International Ash Utilization Symposium, Center for Applied Energy Research, Lexington, Ky., October 20–22, 1997, p. 785–792.

Crowley, S.S., Ruppert, L.F., Belkin, H.E., Stanton, R.W., and Moore, T.A., 1993, Factors affecting the geochemistry of a thick, subbituminous coal bed in the Powder River Basin—Volcanic, detrital, and peat-forming processes: Organic Geochemistry, v. 20, no. 6, p. 843–853.

Ellis, M.S., Flores, R.M., Ochs, A.M., Stricker, G.D., Gunther, G.L., Rossi, G.S., Bader, L.R., Schuenemeyer, J.H., and Power, H.C., 1999, Gillette coalfield, Powder River Basin; Geology, coal quality, and coal resources, Chapter PG of the 1999 resource assessment of selected Tertiary coal beds and zones in the northern Rocky Mountains and Great Plains Region: U.S. Geological Survey Professional Paper 1625–A, p. PG1-PG84. On CD-ROM.

Finkelman, R.B., Breit, G.N., Eble, C., Affolter, R.H., Belkin, H.E., Brownfield, M.E., Cathcart, J.D., Crowley, S.S., Hower, J.C., Leventhal, J.S., McGee, J., Palmer, C.A., Reynolds, R.L., Rice, C.A., and Zielinski, R.A., 1996, Systematic investigation of the compositional variations in solid waste products from coal combustion: American Association of Petroleum Geologists, Eastern Section, October 12–16, 1996, p. 39–40.

Finkelman, R.B., Colker, Allan, and Palmer, C.A., 1997, Modes of occurrence of arsenic and other trace elements in fly ash from a Kentucky power plant: Proceedings of the 1997 International Ash Utilization Symposium, Center for Applied Energy Research, Lexington, Ky., October 20–22, 1997, p. 239–246.

Finkelman, R.B., Palmer, C.A., Krasnow, M.R., Aruscavage, P.S., and Sellers, G.A., 1990, Heating and leaching behavior of elements in the eight Argonne Premium Coal Samples: Energy and Fuels, v. 4, no. 6, p. 755–767.

Fishman, N.S., Rice, C.A., Breit, G.N., and Johnson, R.D., 1999, Sulfur-bearing coatings on fly ash from a coal-fired power plant—Composition, origin, and influence on ash alteration: Fuel, v. 58, p. 187–196.

Fleischer, Michael, 1987, Glossary of mineral species: Tucson, Ariz., The Mineralogical Record, Inc., 227 p.

Gluskoter, H.J., 1965, Electric low-temperature ashing of bituminous coal: Fuel, v. 44, p. 285–291.

Gluskoter, H.J., Ruch, R.R., Miller, W.G., Cahill, R.A., Dreher, G.B., and Kuhn, J.K., 1977, Trace elements in coal—Occurrence and distribution: Illinois Geological Survey Circular 499, 154 p.

Hower, J.C., Trerice, D.R., Graham, U.M., Groppo, J.G., Brooks, S.M., Robl, T.L., and Medina, S.S., 1995, Approaches to the petrographic characterization of fly ash: Proceedings of the 11th International Coal Testing Conference, Center for Applied Energy Research, Lexington, Ky., May 1995, p. 49–54.

International Centre for Diffraction Data, 1999, Powder diffraction file (PDF-2): International Centre for Diffraction Data, 12 Campus Boulevard, Newtown Square, PA 19073 U.S.A.

Larson, A.C., and Von Dreele, R.B., 1994, General structure analysis system (GSAS): Los Alamos National Laboratory Report LAUR 86-748, 231 p.

Lauf, R.J., Harris, L.A., and Rawlson, S.S., 1982, Pyrite framboids as the source of magnetic spheres in fly ash: Environmental Science and Technology, v. 16, p. 218–220.

McCarthy, G.J., Solem, J.K., Bender, J.A., and Eylands, K.E., 1993, Mineralogical analysis of advanced coal conversion residuals by X-ray diffraction: Proceedings of the Tenth International Ash Use Symposium, American Coal Association, EPRI TR-101774, p. 58-1–58-12.

O'Connor, J.T., 1997a, Silicate fly ash classification based on exsolution mineralogy: Proceedings of the 1997 International Ash Utilization Symposium, Lexington, Ky., October 20–22, 1997, p. 692–699.

O'Connor, J.T., 1997b, U- and F-bearing phosphate-silicate fly ash grains: Proceedings of the 1997 International Ash Utilization Symposium, Center for Applied Energy Research, Lexington, Ky., October 20–22, 1997, p. 716–721.

O'Connor, J.T., and Meeker, G.M., 1999, Liquidus (Ca+Mg)-rich exsolution phases in low-sulfur fly ash: Proceedings Volume of the 24th International Technical Conference on Coal Utilization and Fuel Systems, Clearwater, Fla., March 8–11, 1999, p. 333–342.

Palache, Charles, Berman, Harry, and Frondel, Clifford, 1951, Dana's System of Mineralogy, Seventh Edition: New York, John Wiley, 1124 p.

Palmer, C.A., and Filby, R.H., 1984, Distribution of trace elements in coal from the Powhatan No. 6 Mine, Ohio: Fuel, v. 63, p. 318–328.

Palmer, C.A., Mroczkowski, S.J., Kolker, Allan, Finkelman, R.B., and Bullock, J.H., Jr., 2000, Chemical analysis and modes of occurrence of selected trace elements in a Powder River Basin coal and its corresponding simulated cleaned coal: U.S. Geological Survey Open-File Report 00-323, 52 p.

Palmer, C.A., Mroczkowski, S.J., Kolker, Allan, Finkelman, R.B., Crowley, S.S., and Bullock, J.H., Jr., 1998, The use of sequential leaching to quantify the modes of occurrence of elements in coal: Fifteenth Annual International Pittsburgh Coal Conference Proceedings, Pittsburgh, Pa., September 15–17, 1998, CD-ROM, PDF 166, 28 p.

Querol, X., Fernadez-Turiel, J.L., and Lopez-Soler, A., 1995, Trace elements in coal and their behavior during combustion in a large power station: Fuel, v. 74, no. 3, p. 331–343.

Rice, C.A., Breit, G.N., Fishman, N.S., and Bullock, J.H., Jr., 1999, Leachability of trace elements in coal and coal combustion products: The Proceedings of the 24th International Technical Conference on Coal Utilization and Fuel Systems, Clearwater, Fla., March 8–11, 1999, p. 355–366.

Rice, C.A., Breit, G.N., Fishman, N.S., Bullock, J.H., Jr., and Motooka, J., 1997, Geochemical analysis and modeling of coal combustion waste leaches: Proceedings of the 1997 International Ash Utilization Symposium, Center for Applied Energy Research, Lexington, Ky., October 20–22, 1997, p. 231–238.

Stach, E., Mackowsky, M.-Th., Teichmüller, M., Taylor, G.H., Chandra, D., and Teichmüller, R., 1982, Stach's textbook of coal petrology: Berlin, Gebrüder Borntraeger, 535 p.

Starkey, H.C., 1984, Sodium hypochlorite as an aid to the extraction of clay minerals from black shales, *in* Bush, A.L., ed., Contributions to mineral resources research, 1984: U.S. Geological Survey Bulletin 1694, p. 75–80.

Schlorholtz, S., Bergeson, K., and Derirel, T., 1988, Monitoring of fluctuations in the physical and chemical properties of a high-calcium fly ash, *in* Fly ash and coal conversion by-products—Characterization, utilization and disposal IV: Materials Research Society Symposium Proceedings, v. 113, p. 99–106.

Triplehorn, D.M., Stanton, R.W., Ruppert, L.F., and Crowley, S.S., 1991, Volcanic ash dispersed in the Wyodak-Anderson coal zone, Powder River Basin, Wyoming: Organic Geochemistry, v. 17, no. 4, p. 567–575.

U.S. Statutes at Large, 1990, Provisions for attainment and maintenance of National ambient air quality standards: Public Law 101-549, 101st Congress, 2nd Session, v. 104, pt. 4, p. 2353–3358.

Zielinski, R.A., and Finkelman, R.B., 1997, Radioactive elements in coal and fly ash—Abundance, forms, and environmental significance: U.S. Geological Survey Fact Sheet FS-163-97, 4 p.